MSc Thesis Report

Exploring Electrochemical Disinfection for Decentralized Drinking Water Production:

from Laboratory Research to Field Application in Ghana

Carolina Nanni

Delft University of Technology

TU Delft

MSc Thesis Report

Exploring Electrochemical Disinfection for Decentralized Drinking Water Production:

from Laboratory Research to Field Application in Ghana

by

Carolina Nanni

Student Name	Student Number
Carolina Nanni	5608945

Chair:	Prof. dr. ir. Doris van Halem
External Supervisor:	Dr. ir. David A. Vermaas
Daily Supervisor:	Ir. Silvy Rijsdijk
Daily Supervisor:	Ir. Shreya Trikannad
Faculty:	Faculty of Civil Engineering and Geosciences, Delft
Defended on:	20th June 2024

Contents

Acknowledgements

This report collects a now year long effort in the final step to attaining the Master's in Science Degree in Civil Engineering (track-Environmental Engineering). It has been an intense, dynamic and bustling year between the TU Delft lab, an incredible trip to Ghana, a short outing to Ghent, and a lot of little adventures in between. To all the people who helped, supported and made all this possible I express my sincere gratitude.

First, I would like to thank my supervisors. Silvy Rijsdijk, for explaining the realms of electrochemistry and steering me through the complications of thesis, but also for being an amazing travel companion and lab buddy through Ghana. That trip will be long remember with joy. The office coffees and little chats while debating electrochemical questions also helped thesis run smoother (and with tastier coffee!) Doris van Halem, for your unwavering enthusiasm and many inspiring outlooks on the thesis which helped me develop the research. Thank you for supporting my plans for Ghana from day 1. Shreya Trikannad, for helping me out in the lab with all the nooks and crannies of bacteria and virus techniques. David Vermaas, for providing valuable external input on electrochemistry which helped make the thesis richer. Furthermore, Guus Wiersma for being our guide in Ghana and showing us all the best spots. Korneel Rabaey, thank you for letting us borrow the Magneli reactor which was an essential asset in this thesis.

I would also like to thank the TU Delft Waterlab staff, for helping me out both in the TU lab and to arrange the fieldwork in Ghana. Your insight made the preparations infinitely easier. I would like to thank the drinking water team for providing valuable feedback during the meetings which helped me improve further.

Lastly, I would like to thank all the people who made my study years so special.

To all the splendid people I've met during my studies in the Netherlands and shared unforgettable moments, from Chile to Greece and here in the Netherlands. Never could I have imagined that these years would be so eventful, colourful and exciting, and you were all a large part of it.

To my roommates, the old and the new - you provided a little homely feeling throughout these years abroad. Your resilience in listening to all my daily stories has helped me more than you can imagine. To the house by the station - my first friends in a new country and the authors of some of my most cherished moments.

To my roman friends, for having been here from the beginning regardless of how far I choose to move. Thank you for being home every time I return.

To my PoliMi friends, with whom I started my university years and who made sure even the darkest *sessione d'esami* was tackled with laughter, humour and celebratory spritz for every accomplishment (and failure).

Last but not least - to my family, my parents and my sisters, for supporting me from the beginning and guiding me back on track when I lose my footing. Your little phone calls during thesis to check in were valuable moments. To Lizzy and Kimby for always making sure life doesn't get too serious.
Matteo - thank you for being a solid anchor and reminding me to keep fun, joy and a little play in everything I do.

A heartfelt thank-you to all the people who've helped and who I met along the way. You made every experience richer, and I learned something from each of you.

Carolina Nanni
Delft, June 2024

Abstract

Decentralized drinking water production continues to face challenges in achieving acceptable standards for human consumption. This is mainly due to difficulty in developing treatments that can operate effectively in low-resource settings, either due to complications associated with providing the system in a decentralized context or overall unsatisfactory performance of the technology adopted. Electrochemical systems are emerging technologies within decentralized settings which provide many advantages to being adapted in resource-limited areas. This study focuses on understanding the mechanisms behind the electrochemical disinfection for the treatment of surface water. Laboratory experiments were conducted to evaluate the performance of an RuO_2/IrO_2 and a Magneli-phase reactor for the disinfection of a bacteria species, *Escherichia Coli*, and a virus species, ΦX174. The two reactors are characterised in terms of distinct anodic properties and their performance is assessed by promoting different electrochemical reactions for the generation of various disinfectant agents within the electrochemical cell, with specific focus on the formation of chlorine and Reactive Oxygen Species (ROS). Chlorine-based disinfection proved to be the primary agent in the removal of both pathogens; a 4 log removal for *E. Coli* was achieved at an energy use of 0.41 kWh/m^3 for RuO_2/IrO_2 and of 0.31 kWh/m^3 for Magneli, and a 5 log removal for ΦX174 was achieved at 2.88 kWh/m^3 for RuO_2/IrO_2 and for 1.18 kWh/m^3 for Magneli.

To further assess the viability for the treatment of surface waters in decentralized settings, the RuO_2/IrO_2 was also tested in a field setting in Ghana making use of different water types to compare the utility in using an electrochemical reactor to produce chlorine for disinfection as compared to traditional disinfection methods. Seawater, lagoon and river water were tested, achieving an energy use per gram of produced chlorine of 0.007, 0.046 and 0.066 $kWh/g_{chlorine}$ for a produced chlorine dose of 35 mg/L for seawater and 5 mg/L for the lagoon and river water. With these results, chlorine can be produced from river water at an equivalent dosage to traditional chlorine tablets, and at a cost that is 40 times lower.

List of Figures

List of Tables

Abbreviations

BDD Boron Doped Diamond [electrodes]

CAPEX Capital Expenditures

CER Chlorine Evolution Reaction

CFU Coliform Forming Unit

DBPs Disinfection By-Products

ED Electrochemical Disinfection

EC Electrical Conductivity

HRT Hydraulic Retention Time

LRV Log Removal Value

NTU Nephelometric Turbidity Units

OER Oxygen Evolution Reaction

OPEX Operational Expenditures

ORP Oxidation Reduction Potential

POU Point-of-Use

PFU Plaque Forming Unit

ROS Reactive Oxygen Species

1

Introduction

1.1. Background

According to the World Health Organization (WHO), two billion people lack access to safe drinking water as of 2020, of which 8 out of 10 reside in rural and decentralized areas. The major issue is in Sub-Saharan Africa, where only 64% of the population has access to at least basic drinking water services [39] [19]. Microbial contamination of drinking water poses the greatest risk to drinking water safety, with an estimated 4000 people dying every day from diseases connected to inadequate water, sanitation, and hygiene conditions [73].

The main difficulty with providing pathogen-free drinking water in rural areas are the high capital and maintenance costs and the transportation and storage of disinfectant reagents, which makes the implementation in decentralized settings complex and oftentimes inefficient in the long run [114]. Furthermore, rural areas often lack access to the centralized treatment line and rely instead on available boreholes and wells for water, which makes Point-of-Use (POU) technologies a more feasible solution for water treatment [84]. Within resource-limited settings, disinfection at the POU is often achieved with technologies such as filters and coagulant/oxidants sachets, which however demonstrated lower removal efficiency to conventional treatment methods (0.5-2 log removal for POU technologies as compared to 3 log removal of chlorination, ozonation and UV systems) and therefore insufficient protection against pathogen exposure [33].

Therefore, there is a critical demand to develop disinfection technologies for decentralized systems that are reliable, effective in removing pathogens, inexpensive and easy to use [49]. Electrochemical Disinfection (ED) has gained growing interest in recent years as an alternative to chemical disinfection for the treatment of water. In ED, disinfectants are generated in-situ through anodic electrochemical reactions, bypassing the need for transport and storage of hazardous chemicals and allowing to scale the chemical dosing to the requirements in loco [33] [5] [44]. ED has proven efficient for a wide range of microorganisms, is easy to install and can be operated through compact mobile units. Lastly, the operational energy requirements are relatively low and studies have proven the possibility of adopting photovoltaic systems to operate electrochemical systems far from the electric supply grid [114] [26]. Where POU technologies are adopted, discontinuous operation is usually required, and electrochemical systems have demonstrated reliability in operating on/off cycles [96]. All these factors make ED a promising solution for decentralized systems [49].

As of 2024, literature indicates an increase in research on ED, which has been tested and applied to different water sources. Substantial literature focuses on the generation of different disinfectant agents, mainly active chlorine and Reactive Oxygen Species (ROS), but increasing literature is also focusing on alternative disinfectant types, and exploring the mechanisms which enhance the formation of specific disinfectant agents is a focus [48]. A large number of experiments focus on developing chlorine-free disinfection systems that achieve comparable removal efficiencies with similar energy use. From an operational perspective, new tendencies include increasing the disinfection efficiency with different electrode types and the creation of hybrid technologies to meet the demands of field settings and mimic full-scale disinfection plants [10].

1.2. Disinfection by Chlorine

Chlorine is widely used as disinfectant in field applications and POU technologies due to its fast action, reliability and long-term residual effect. When added to the water, chlorine will react with the pathogens and kill them. The chlorine remaining after some time from initial dosing is the residual chlorine, which is the unreacted chlorine that provides protection against re-contamination. This allows water treated by chlorine to be safely stored and distributed to consumers. Chlorine also reacts with the organic matter present in the water, so when water contains turbidity (measured in Nephelometric Turbidity Units (NTU)), sufficient chlorine has to be dosed to ensure that the desired residual chlorine concentration is maintained throughout the system. However, over-chlorination must be avoided as it gives the water an unpleasant odour and taste, is harmful to aquatic life and enhances the production of toxic Disinfection By-Products (DBPs)[82] [1]. Diagram 1.1 summarizes the connection between chlorine dose and chlorine residual.

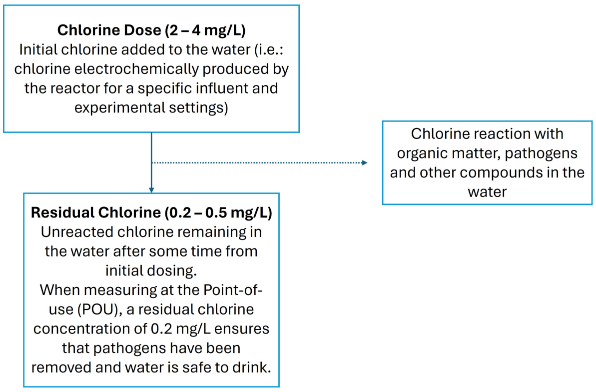

Chlorine Dose (2 – 4 mg/L)
Initial chlorine added to the water (i.e.: chlorine electrochemically produced by the reactor for a specific influent and experimental settings)

Chlorine reaction with organic matter, pathogens and other compounds in the water

Residual Chlorine (0.2 – 0.5 mg/L)
Unreacted chlorine remaining in the water after some time from initial dosing.
When measuring at the Point-of-use (POU), a residual chlorine concentration of 0.2 mg/L ensures that pathogens have been removed and water is safe to drink.

Figure 1.1: Transition from chlorine dose to chlorine residual. Recommended values for both chlorine forms are indicated. The maximum chlorine concentration in water for human consumption is 5 mg/L, according to the WHO.

The WHO [74] set standards for chlorine disinfection in POU technologies based on the quality of the influent water to ensure a sufficient residual chlorine of 0.2 mg/L in stored household water treated by chlorination. The recommendations are to dose *clear water* (turbidity < 10 NTU) with 2 mg/L of chlorine, and *turbid water* (turbidity > 10 NTU) with 4 mg/L. These standards are used as reference in this research.

1.3. Electrochemical Oxidation as a disinfection method of surface water

The working principle of electrochemical systems as a disinfection technology is the production of oxidising disinfectants through anodic oxidation processes and the oxidation of bacteria directly at the anode surface. These processes occur when electric energy is provided via the current i [A] to electrodes immersed in aqueous suspensions containing microbes [20] [53]. This prompts a charge transfer through the system which determines which reactions can occur, which depends on the electrode potential ($E_{\text{electrode}}$) acquired from the provided i. For a specific reaction to occur, the $E_{\text{electrode}}$ must exceed the overpotential of the reaction, which is the additional potential over the thermodynamic requirement (corresponding to the standard electrode potential E^0 of the reaction) that has to be supplied to the electrode to overcome the activation energy of the reaction (equation 1.1). The overpotential depends on the reaction type and electrode properties [109].

$$E_{\text{electrode}} = E^0 + \text{overpotential} \tag{1.1}$$

Three distinct anodic processes facilitate pathogen removal in electrochemical cells: direct oxidation, indirect oxidation and oxidation by ROS.

1.3.1. Direct oxidation

In direct oxidation, pathogens are oxidised through direct contact at the anode surface via electron exchange between the pathogen cells and the anode. Direct oxidation can occur at low potentials before the occurrence of the Oxygen Evolution Reaction (OER), but this oxidation type generally has a low reaction rate, making it limited by kinetics rather than by thermodynamics [60] [15]. At higher potentials, direct oxidation still occurs but its contribution in disinfection is generally outperformed by other disinfection processes.

1.3.2. Indirect oxidation

In indirect oxidation, species present in the water are oxidised at the anode, forming oxidised product with disinfectant capacity which diffuses in the bulk solution. This oxidation type occurs for ($E_{\mathrm{electrode}}$) specific to the contaminant and anode type. The electrochemical production of chlorine species belongs to this type of anodic process, and involves the direct oxidation of chloride ion present in the water to form chlorine gas (equation 1.2), which then hydrolyzes to form hypochlorous acid (HOCl) and hypochlorite ion (OCl^-) (equations 1.3 and 1.4) [33].

$$Cl^- \longrightarrow \frac{1}{2}Cl_2 + e^- \quad E^0 = 1.36\,V/SHE \tag{1.2}$$

$$Cl_2 + H_2O \longrightarrow HOCl + HCl \tag{1.3}$$

$$HOCl \rightleftharpoons ClO^- + H^+ \tag{1.4}$$

The sum of HOCl and OCl^- is referred to as 'free' or 'active' chlorine and represents the key element in chlorine-based disinfection [44]. The equilibrium of the three chlorine species (Cl_2, HOCl and OCl^-) in solution is pH-dependant (Appendix A2) [55]. Literature indicates that HOCl is the strongest disinfectant agent of the chlorine species, resulting up to 80 times more effective for the inactivation of *Escherichia coli* than the equivalent dose of OCl^-, and has been proven most effective for both the removal of bacteria and of viruses. In drinking water disinfection by chlorine, keeping a pH between 6.5 and 7.5 is recommended to maximise disinfection and residual chlorine efficiency [82] [42] [13] [64].

In ED, the facility and cost-effectiveness of electrochemically generating chlorine makes it a favorable disinfection technology. Its use has been extended to swimming pool water and seawater treatment [10] [47].

1.3.3. Oxidation by ROS

ROS are formed by water discharge at the anode, which generates hydroxyl radicals ($OH^\bullet$) (Equation 1.5) from which other ROS are formed (equations 1.6 to 1.8) [61] [92]. $OH^\bullet$ is an intermediate in the OER of water to oxygen. The Appendix (A6.4) provides the full development of the OER.

$$H_2O \rightarrow OH^{\cdot} + H^+ + e^- \quad E^0 = 2.80\,V/SHE \tag{1.5}$$

$$OH^{\cdot} \rightarrow O^{\cdot} + H^+ + e^- \tag{1.6}$$

$$2OH^{\cdot} \rightarrow H_2O_2 + 2e^- \tag{1.7}$$

$$O_2(g) + O^{\cdot} \rightarrow O_3 \tag{1.8}$$

ROS are valuable in ED as they are formed directly from the oxidation of water without any chemical addition required [108]. They are highly reactive, non-selective oxidizing agents which have been used to remove many contaminants in water [72] [16] [76]. In particular, $OH^\bullet$ is recognised as one of the most powerful oxidants generated in electrochemical systems [103].

1.3.4. ED: State-of-the-Art

Through the different anodic oxidation mechanisms, many different oxidants can be formed, and the full spectrum of all occurring oxidation processes is still unclear [10]. The disinfectants most commonly mentioned in literature are the ROS species $OH^\bullet$, hydrogen peroxide (H_2O_2), ozone (O_3), and free chlorine species when chloride ion is present as precursor [20] [53] [100] [81] [108]. Disinfection is defined as ROS-based or chlorine-based respectively [50] [83] [5]. Less frequently, the formation of peroxodisulphate ($S_2O_8^{2-}$) as oxidant is mentioned when sulphate is present as precursor [78] [21] [41]. The disinfectant performance of peroxodisulphate is determined by its decomposition into sulphate radicals ROS (equation A6.4) [67]. Literature has also illustrated the efficiency of bacteria and virus removal through direct oxidation at the anode surface, via direct electron transfer between the anode surface and the microbial cell. This occurs for lower electrode potentials than those required to form oxidising disinfectants[63], but this procedure is time-consuming and literature indicates that direct oxidation alone is not sufficient in reducing the number of pathogens to ensure safely treated water [10, 22]. Figure 1.2 shows an overview of the the main oxidation processes occurring in the anodic cell for this research:

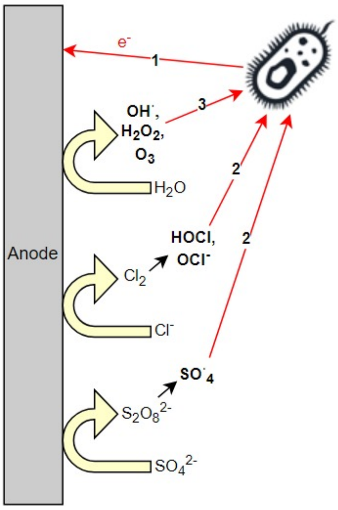

Figure 1.2: Overview disinfection processes occurring in the anodic cell: **(1)** direct disinfection; **(2)** indirect disinfection; **(3)** ROS oxidation

Studies have evaluated the key parameters contributing to disinfection. ROS are highly effective oxidants with efficiency for a high range of microorganisms. Their use in disinfection is preferred to chlorine due to lower DBPs production [35], but their inability to provide residual disinfection effect may determine recontamination during distribution [67] [4]. Regarding $OH^\bullet$, lower dosages are required to achieve equivalent disinfection as chlorine, but their short life and high reactivity with substances in the water inhibit their efficiency[35]. Furthermore, the E^0 of $OH^\bullet$ is twice that of chloride, so higher energy is required to initiate the $OH^\bullet$ oxidation process [33]. Experiments indicate that $OH^\bullet$ are the main performing species in ROS-based disinfection, but their role becomes negligible when chlorine electrolysis is also occurring [35] [81]. For chlorine-based disinfection, the applied current and chloride content are the the most important factors for its performance, with higher chloride content enhancing *E. Coli* disinfection kinetics [79] [81]. Overall, the electrochemical generation of different disinfectant agents is influenced by the water quality and applied electrochemical settings, with the production of one species predominating when conditions are unfavourable for the production of another species [48].

1.3.5. Active and non-Active anodes

The anode material is the most important factor in the efficiency of the ED process, impacting the selectivity of the three oxidation processes, the predominant oxidants formed, and the reaction kinetics [61] [77] [108], [86]. It also affects the overpotentials of the reactions, impacting the energy requirements to produce different species and the competition between reactions occurring on the anode surface [108]. Depending on their material, metal oxide anodes can be of two types: active and non-active [15]. Active anodes exhibit strong interactions between the $OH^\bullet$ formed in equation 1.5 and the electrode surface, determining lower contribution of the formed $OH^\bullet$ ions in the processes occurring in the electrochemical cell. It is suggested that the strong interactions are due to the existence of higher oxidation states of the metals forming the anode, where the adsorbed oxygen species originating from the intermediates of the OER can be incorporated [59]. Non-active anodes have weak interactions between the electrode surface and the $OH^\bullet$, allowing the $OH^\bullet$ to interact with the species in solution [57] [108]. The weaker interaction results in high anode overpotentials for the OER, [58], reducing competition between the OER and the Chlorine Evolution Reaction (CER) which commonly occurs in active electrodes and interferes with the chlorine production [15] [5] [40]. A higher OER overpotential would also suggest a faster $OH^\bullet$ generation kinetics [62] [108]. These aspects would explain why active electrodes have proven to generate insufficient $OH^\bullet$ as compared to non-active electrodes. For this research, one active dimensionally-stable anode (DSA®) and a non-active Magneli-phase type anode were used. The anodes are described in Chapter 2.1.

The ED performance of these anodes in producing chlorine versus ROS-type oxidants for disinfection were compared. Overall, the weaker bonds between the formed $OH^\bullet$ and the anode surface determines that non-active anodes have greater potential in the removal of contaminants via the action of the generated $OH^\bullet$

[57]. Active anodes, particularly DSA®-type electrodes with mixed metal oxides of iridium and/or ruthenium, proved higher chlorine efficiency as compared to other types of metals [44] [61] [47] [54] [36] [90] [113] [3] [106]. For non-active electrodes, a substantial amount of research on Boron Doped Diamond [electrodes] (BDD)confirms their high efficiency in generating $OH^\bullet$ due to their high OER overpotential [79]. Literature relative to Magneli-phase electrodes is more recent. Ti_4O_7 Magneli-phase, as the anode used in this research, has shown to achieve over an order of magnitude higher mass transport rates when operated in flow-through mode as compared to BDD [97]. Of all Magneli-phase electrodes, Ti_4O_7 also have the highest rate of formation of $OH^\bullet$ [111] [51].

An overview of different anode materials and properties is given in Appendix A3.

1.3.6. Pathogenic contamination of surface waters

Human pathogenic viruses are common contaminants in compromised sanitation conditions, and have been found both in drinking water sources and drinking water systems due to pipe leakages or improper wastewater treatment [112]. Despite viruses posing a 10 to 10^4 higher disease risk than bacteria at the same exposure level [32], they are not always included in water quality standards. Organizations use *E. Coli* or total coliform as viral contamination indicators [112], although viruses are more resistant to chemical disinfectants than bacteria [12]. In ED, bacteriophages are 2 to 4 times less sensitive to electric currents than bacteria, with ED generally less effective at removing viruses than bacteria [22] [48]. However, many of the technologies used to treat drinking water were originally designed to remove bacteria [30]. This study uses ΦX174 as an indicator of enteric viruses, and *E. Coli* as bacterial indicator of faecal contamination. Acute gastrointestinal illness caused by enteric viruses is the most commonly reported viral contamination for humans, and faecal contamination is the primary agent in microbial contamination of drinking water [30] [73]. Limited research exists on ΦX174 inactivation by chlorine [112].

The WHO defined log reduction standards for treatment technologies operating at the POU, or household level. The standards, used in this research to evaluate ED performance, recommended three levels of pathogen treatment performance. The highest standard defines a 4 and 5 $\log_{10}$ removal of bacteria and viruses respectively. Technologies that achieve this standard are defined as *highly protective*. The intermediate standard defines *protective* the technologies which ensure a log removal of 2 and 3 respectively for bacteria and viruses. The lowest standard, *interim*, applies to technologies which achieve the *protective* standard for two of three pathogens between bacteria, virus or protozoa [93]. An overview of these standards is provided in Table A7.2.

1.4. Problem Statement

A substantial amount of literature agrees that ED is one of the most promising alternatives which can be installed as a decentralized disinfection system in rural areas. However, literature is still contrasting on the full functionality of the system. The effect of different boundary conditions (water parameters, electrode type, different ED techniques) is still unclear, as well as the parameters required to fully optimise the system. More research can be found in the treatment of wastewater or industrial effluents, whilst the functionality of the system when dealing with drinking water sources, which have lower conductivity and different degrees of pollution, has been less explored. Furthermore, there is a lack of research, experiments and testing of the performance of an ED system in a rural setting, where POU technologies for the treatment of water can provide suitable treatment alternatives to centralized approaches.

1.5. Research Questions

The aim of this research is twofold. The first part is dedicated to comparing the performance of two distinct electrochemical reactors in the controlled settings of a lab. The differences which characterise the two reactors are presented in chapter 2.1. Electrochemical disinfection and how it is occurring in the two reactors is also investigated, with the purpose of using the reactor as a POU technology in decentralized settings. Research questions 1 and 2 are focused on this topic. The second part explores the performance of one of the electrochemical reactors for the production of chlorine species in a field setting (research question 3).

Research Question 1: How do the performances of the RuO_2/IrO_2 and Magneli reactors compare in terms of chlorine production and energy consumption?

Research Question 2: Which processes are contributing to the electrochemical disinfection occurring in the RuO_2/IrO_2 and Magneli reactors?

Research Question 3: What is the impact of using real water sources to produce chlorine species while operating the RuO_2/IrO_2 reactor in a field setting in Ghana?

This report is organised as follows. Chapter 2 will give a description of the experimental set-up used for the experiments in the lab and in the field, as well as the materials used for this research. Chapter 3 will present the results of the experiments. Chapter 4 will discuss the results. Lastly, Chapter 5 will present the conclusions and future recommendations.

2

Materials and Methods

In this chapter the used materials and the followed methods are described. The experimental set-up and the operation of an electrochemical cell are described in single chapters. The experimental settings, materials used and procedures followed for sampling and analysis are subdivided into sections to distinguish between the methods used in the lab and in the field.

2.1. Experimental Set-up

The experimental set-up consisted of a flow through, flat-plate electrochemical reactor comprising of two chambers in perspex frames separated by an monovalent cation exchange membrane (CEM). Two mesh-like electrodes, an anode and a cathode, were enclosed in the two separated chambers and connected to a DC power supply (30V-3A TENMA 72-10500 bench DC power supply) via crocodile clip cables. As the reactor was operated in flow-through mode, the separate influent of the cathode and anode was fed to the bottom of the chambers via peristaltic pumps (Watson Marlow 120U). The CEM prevented the mixing of the anode and cathode solution while allowing monovalent cations to pass the membrane.

For the first part of the research, experiments were conducted in the TU Delft Waterlab. In this setting, two different electrochemical reactors were used; one consisting of an active anode and one of a non-active anode. The two reactors differed in anode material and in the volumes of the anode and cathode chamber.
The active anode (hereafter referred to as *RuO_2/IrO_2*) was a Ti mesh coated with RuO_2/IrO_2. The volumes of the chambers were of 200 m^3. The non-active anode (hereafter referred to as *Magneli*) was a Magneli-phase Ti_4O_7-coated anode. The chamber volumes were of 95 m^3. The surface area of both anodes was 100 cm^2. For both reactors, a stainless steel mesh (100 cm^2) was used as cathode.
In this set-up, the anode and the cathode had two distinct feed solutions contained in 10L jerrycans. The effluent from the two chambers was collected separately in 10L jerrycans. When performing disinfection experiments, the anode feed water was continuously stirred using a magnetic stirrer (Labinco).

For the second part of the research, experiments were conducted in a field setting located by the Kpeshie Lagoon in Accra, Ghana. Only the RuO_2/IrO_2 reactor was used for these experiments. In this set-up, the anode and cathode were supplied the same feed solution from a 15L plastic bottle, pumped to the separate chambers via two peristaltic pumps. The effluent was directed to two separate 15L plastic bottles. To keep the organics in the feed water distributed uniformly throughout the experiments, the bottle was shaken every five minutes.

For both set-ups, the effluent from the anode chamber was collected for further analysis. As a result of water electrolysis taking place in the electrochemical reactor, H_2 gas was produced as a side-reaction at the cathode, whilst O_2 gas was produced at the anode. In experiments where chloride was present in the system, Cl_2 gas was also produced at the anode. The gases left the system and were not collected for analysis.

Schematic diagrams of the set-ups are provided in Figure 2.1a for the experiments conducted in the lab and in Figure 2.1b for the experiments conducted in the field. Pictures of both set-ups are also provided in the A9.

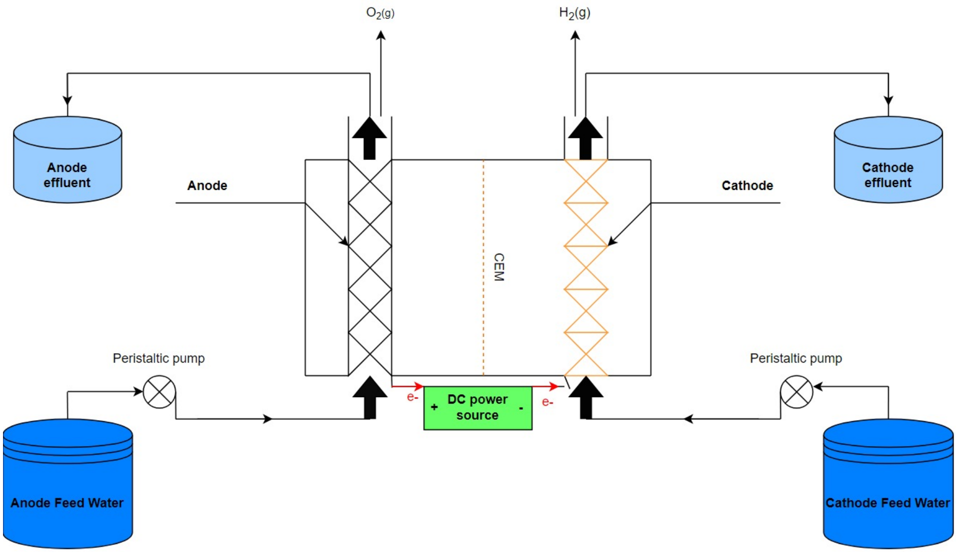

(a) Laboratory Set-up

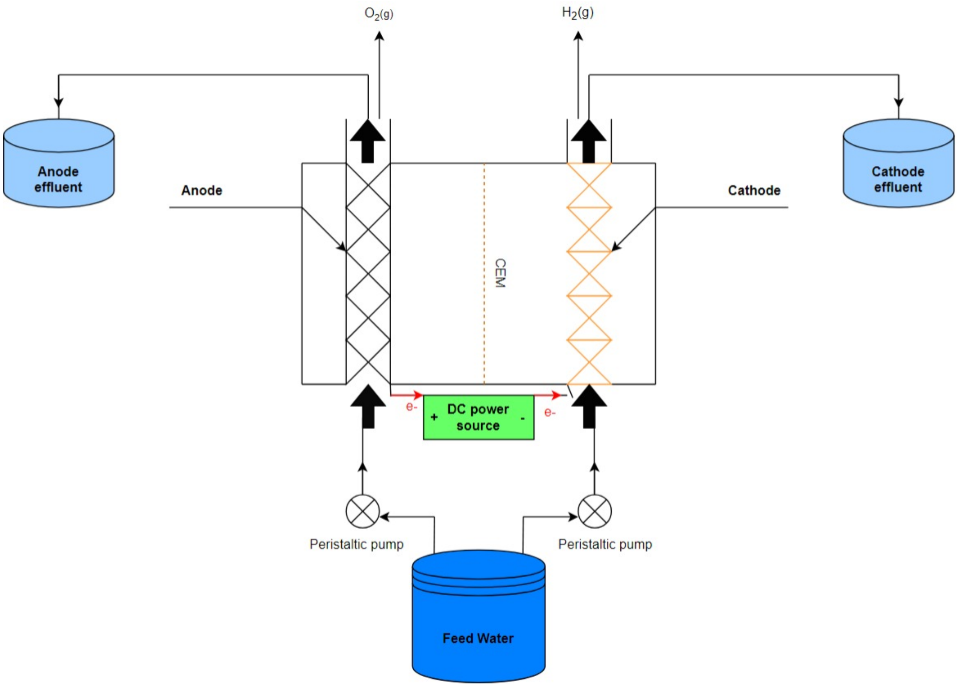

(b) Field Set-up

Figure 2.1: Experimental set-ups for the Electrochemical disinfection experiments

2.2. Electrochemical cell operation

The operation of the electrochemical reactor and the anodic performance in electrochemical disinfection depends on the applied operational settings and water matrix characteristics, including pH, electrolyte and pollutant concentration [33] [83] [77].

The applied current density i [A/m^2: C/s/m^2] was measured by dividing current I [A] supplied by the DC power source with the electrode surface (equation 2.1), and represents the charge [C] passed in the unit of time [s] through the electrode surface [m^2] [43].

$$i[A/m^2] = \frac{I}{0.01} \tag{2.1}$$

The reactors were operated in continuous flow-through mode. The operational flow rates were chosen to provide the system a set charge dosage (q) [C/L] (equation 2.2), which is the charge [C] given to the unit volume of water [L] and is obtained by dividing the supplied current by the flow rate [L/s].

$$q\left[\frac{C}{L}\right] = \frac{I[A]}{Q\left[\frac{L}{s}\right]} = \frac{I \times HRT[s]}{\text{Reactor Volume}[L]} \tag{2.2}$$

Faradaic efficiency

The Faradaic efficiency [%] is a product yield on an electron basis and is used to measure the electrochemical selectivity of a reaction. The Faradaic efficiency is calculated as the ratio between the actual moles of product generated, calculated via analytic methods, and the theoretical mole of product generated from the consumed charge, as given in equation 2.3.

$$\text{Theoretical product generated [mole/L]} = \frac{q}{Na \times e \times n} \tag{2.3}$$

Where:

$$\begin{aligned} &q: \text{ charge dosage } [C/L] \\ &Na: \text{ Avogadro constant } [1/mol] = 6.02214 \times 10^{23} \\ &e: \text{ elementary charge } [C] = 1.6022 \times 10^{-19} \\ &n: \text{ number of electrons transferred during oxidation } [-] \end{aligned}$$

Energy and resistance of the electrochemical cell

The energy consumption (in kWh/m^3) of the electrochemical oxidation process was obtained from the cell voltage (V) [V] and the applied charge dosage q [C/L] through equation 2.4.

$$\text{Energy [kWh/m}^3\text{]} = \frac{V \cdot q}{3.6 \times 10^3} \tag{2.4}$$

The cell resistance (R) during the operation of the cell is function of the cell voltage and applied current density I [A] according to equation 2.5:

$$R = \frac{V}{I} \tag{2.5}$$

2.3. Experimental Settings

Preliminary experiments were conducted on the RuO_2/IrO_2 with two objectives: identify the operational conditions which ensured the WHO recommended chlorine dose for turbid water of 4 mg/L free chlorine, and identify the operational q which ensured a weakly acidic effluent pH.

From the results of the preliminary experiments, a q of 300 C/L was selected. Experiments were performed on the RuO_2/IrO_2 and Magneli by operating the reactors under the same working conditions (Charge Dosage, q [C/L], Current Density, i [A/m^2] and flow through the reactor, Q [m^3/s]) to determine the operation and performance differences in the two reactors. For the experiments focused on electrochemical disinfection, it was decided to choose four experimental settings to evaluate the variation in pathogen removal for changing electrochemical settings. The chosen settings are shown in Table 2.1. Settings 1, 2 and 3 were adopted for both *E. Coli* and ΦX174 removal. Setting 4 was used only for ΦX174 removal due to the ΦX174 initial concentration being 2 logs higher than *E. Coli*.

All the experiments were performed in duplicates. An overview of each experimental data-point, along with the corresponding Hydraulic Retention Time (HRT) for each reactor is presented in A4.1, A5.1 and A7.1.

Setting *E. Coli*	Setting ΦX174	Charge Dosage [C/L]	Current Density [A/m^2]
E1	ϕ_1	150	16.7
E2	ϕ_2	300	16.7
E3	ϕ_3	300	33.3
-	ϕ_4	600	33.3

Table 2.1: Experimental settings for disinfection experiments

2.4. Materials

2.4.1. Materials: Laboratory experiments

Influent water

The influent water used for the laboratory experiments consisted of demineralised water with the addition of sodium chloride (NaCl) as electrolyte for the chlorine-based experiments, and of sodium sulphate (Na_2SO_4) for the ROS-based experiments, to concentrations resembling tap water. The two electrolytes were dosed separately to evaluate the contribution of different factors in disinfection. The NaCl was added in the chlorine-based experiments to provide the chloride ion needed for chloride oxidation to chlorine. In the ROS-based experiments, the addition of Na_2SO_4 was required to reach the desired water conductivity and create a chlorine-free environment to observe disinfection by means of ROS species. In addition, sodium bicarbonate, $NaHCO_3$, was added to both experiments as pH buffer. The ion composition and conductivity [μS/cm] (averaged over all experiments) of the feed water is given in Table 2.2:

Constituent	Chlorine-based experiments [mg/L]	ROS-based experiments [mg/L]
Cl^-	50	-
$SO_4{}^2-$	-	50
HCO_3	170	170
conductivity [μS/cm]	~460	~380

Table 2.2: Influent water matrix

The Pathogens

The influent water was spiked separately with bacteria (*Escherichia Coli WR1*) and virus (ΦX174) indicators to analyse the impact of ED on different pathogens. Bacteria cell counts are described as Coliform Forming Unit (CFU) while virus cell counts are called Plaque Forming Unit (PFU).

Escherichia Coli (*E. Coli*) is widely used as an indicator of enteric bacteria in drinking water studies [98]. *E. Coli* was dosed to an influent concentration of 10^4 CFU/mL. ΦX174 is a bacteriophage commonly used as an indicator of viral contamination in water [65]. It belongs to the category of coliphages, a subgroup of bacteriophages that infect *E. Coli*, thus it is also used to assess the presence of human enteric viruses [70], [91]. ΦX174 was spiked in the influent water to a concentration of 10^6 PFU/mL.

2.4.2. Materials: Field experiments

Three different water types were collected for the experiments conducted on the field: lagoon water, river water, and seawater.

The lagoon water was collected from the Kpeshie Lagoon in Accra, Ghana. The Kpeshie lagoon is located close to the sea and is subject to seawater infiltration, making the water of brackish quality (EC>15 ms/cm)[89]. Samples for this research were collected close to the lagoon bank.
The river water was collected from the Densu river bank around 30 km from where the Densu discharges in the sea (Weija Gbawe Municipal).
The seawater was collected on Labadi Beach in Accra.

E. Coli was measured in the influent for the lagoon ($<10^2$ CFU/mL) and seawater (no coliform forming units observed). *E. Coli* was not measured for the river water as experiments were performed 48 hours after collecting the water, therefore die-off had occurred. An overview of the characteristics of the collected water samples is given in A7.3.

2.5. Sampling

Samples for all experiments were collected every 3HRTs to ensure stabilization in system performance. For both ROS-based and chlorine-based experiments, 15mL samples were collected to measure the pH and Oxidation Reduction Potential (ORP) of the effluent. For chlorine-based experiments, an additional 10mL sample was collected to measure the effluent chlorine (referred to as *chlorine residual* if the influent water was spiked with pathogens and as *chlorine dose* otherwise). For disinfection experiments, samples were collected to be later used for pathogen enumeration, as described in section 2.6.

For the chlorine-based experiments, the residual chlorine was neutralised in the sample used for enumeration by adding sodium thiosulphate, to prevent further disinfection occurring before plating. Sodium thiosulphate rapidly reacts with chlorine compounds and is a preferred solution to dechlorinate samples in disinfection experiments as it is not toxic to most microorganisms [34]. The reaction between sodium thiosulphate and chlorine compounds generates different products depending on conditions such as pH and dechlorinator dose. For the conditions traditionally used in disinfection, the occurring reaction is given in equation (2.6):

$$2\,\mathrm{Na_2S_2O_3} + \mathrm{Cl_2} \rightleftharpoons \mathrm{Na_2S_4O_6} + 2\,\mathrm{NaCl} \tag{2.6}$$

2.6. Analysis

For all experiments, the electrical conductivity (EC) of the influent and the pH and ORP of both influent and effluent was measured using three probes: TentraCon® 925 (EC), SenTix® ORP-T 900 (ORP) and SenTix® 940 (pH). The cell voltage [V] was recorded for each experiment. The anode potential was not directly measured in this research.

2.6.1. Analysis: Laboratory experiments

The produced chlorine was measured using the free chlorine test kit (Spectroquant®, 0.010-6.00 mg/L Cl2 and theSpectroquant® NOVA 60). The measurements were performed against a blank test to correct for disturbances by NaCl.

E. Coli and ΦX174 enumeration was performed by using the spread plate technique. *E. Coli* was incubated on Chromocult® Coliform Agar plates for 24 h at 37°C. For water samples larger than 0.3 mL, the membrane filter method was used (Whatman® cellulose acetate membrane filters, 0.45 μm). ΦX174 was prepared and assayed according to protocol ISO 10705-2.

2.6.2. Analysis: Field experiments

The water turbidity was measured using Sper Scientific 860040. The produced chlorine was measured using the free chlorine tablets (DPD 1 range 0.02 - 6 mg/L Cl2 and Lovibond MD 600). The measurements were performed against a blank test. *E. Coli* enumeration was performed by pipetting 1mL of sample on dry plates (CompactDry™ EC) and incubating for 24 h (Cultura® M). Virus enumeration was not performed.

2.6.3. Quantification of microbial removal

Microbial removal can be presented in percentages or logarithmic removal values [102]. The latter is used in this research.

The LRV expresses concentrations in terms of order of magnitude and is commonly used to evaluate the variation of higher pathogenic concentrations. Formula 2.7 shows how to calculated the LRV.

$$\text{LRV} = \log_{10}\left(\frac{C_{\text{in}}}{C_{\text{out}}}\right) \tag{2.7}$$

For E. Coli, the maximum volume collected for analysis was 100mL, on the basis of the WHO standards determining that a water is safe for human consumption if 0 CFU are detected in a 100mL water sample. When no CFU were detected in the water collected after treatment, the pathogen count was considered below detection limit. The LRV is indicated as being higher than the maximum value that could be obtained given the *E. Coli* concentration of the water influent C_{in}, and the minimum detectable value of 1 CFU in 100 mL C_{out}. The same is done with *PhiX*, with the minimum detectable value being 1 PFU in 1 mL of sample.

It should be noted, the dry plates used for the field experiments only allowed to analyse 1mL of sample. This posed limitations on the microbial analysis which could be performed in the field, as the low initial *E. Coli* concentrations detected in the brackish lagoon were already removed at the lowest electrochemical settings. As such, considerations on the field experiments focused on the chlorine production rather than on the pathogenic removal.

3

Results

This chapter presents the results of the experiments conducted in the TU Delft laboratory and in the field, in Ghana. The first section shows results relative to the chlorine production of the two reactors, RuO_2/IrO_2 and Magneli, when using demineralized water containing chloride electrolyte. The second section presents the results relative to the electrochemical disinfection of *E. Coli* and ΦX174 with chloride and sulphate electrolytes. The last section reports the results of the electrochemical chlorine production when using the RuO_2/IrO_2 reactor with different water sources in Ghana.

3.1. Performance of RuO_2/IrO_2 and Magneli for chlorine production

This section presents the results of the experiments conducted on the RuO_2/IrO_2 and the Magneli reactors operated at a constant q =300 C/L and increasing i [A/m^2].

3.1.1. Chlorine Production

Figure 3.1 shows the chlorine production of the RuO_2/IrO_2 (in blue) and Magneli (in orange) reactors. Results are given for i between 4 and 55 A/m^2 for RuO_2/IrO_2, and for i between 7.9 and 52 A/m^2 for Magneli. The chlorine plateau reached for each reactor are also highlighted.

The chlorine produced by each reactor increases with increasing i, following an almost identical trend for both reactors. At lower i, the Magneli slightly underperforms as compared to the RuO_2/IrO_2, whilst for higher i the reactors show a similar chlorine output. For increasing i, the chlorine produced by the RuO_2/IrO_2 increases steadily, while the Magneli has larger oscillations. The chlorine production plateau are reached for the RuO_2/IrO_2 at i =40 A/m^2, for 9.22 mg/L chlorine, and the Magneli at i =47 A/m^2 for 10.18 mg/L chlorine. [1]

---

[1] The data-points in Figure 3.1 are sampled every 30 minutes for the RuO_2/IrO_2 and every three HRTs for the Magneli. During a separate experiment, the chlorine production observed after three HRTs at i =33.3 A/m^2, q =300 C/L on the RuO_2/IrO_2 (data-point not shown in Figure) did not show the value expected from the trend observed on the curve. Therefore, additional experiments at three different i were conducted on both reactors to observe if significant differences in chlorine production are present when sampling for the two different time-steps. A slight decrease is reported when sampling every 3 HRTs for the RuO_2/IrO_2 for two of the i tested, whilst values for the Magneli remain congruous for both sampling times. The reason for the described behaviour of the RuO_2/IrO_2 is unknown. Results and values for the two sampling times are given in Appendix A4.1

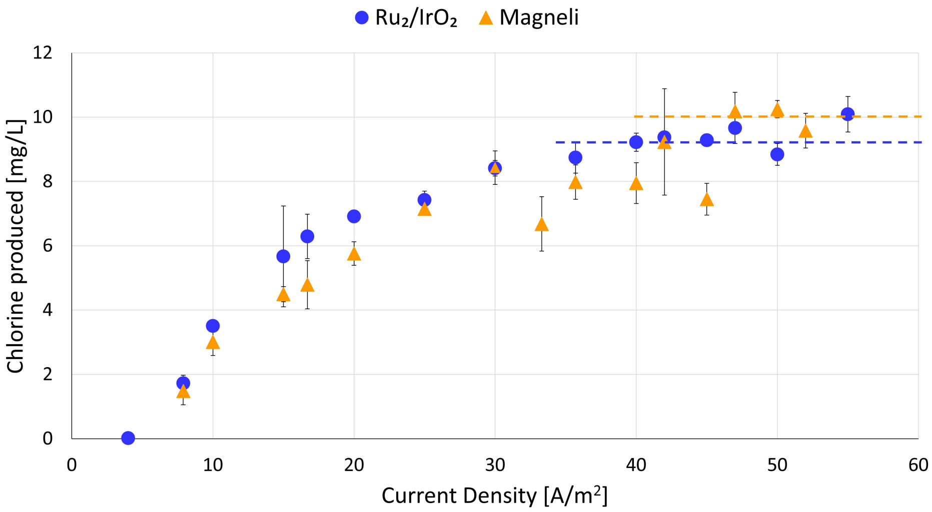

Figure 3.1: Chlorine production for RuO_2/IrO_2 and Magneli reactors operating at constant q =300C/L and increasing i [A/m^2].

3.1.2. Voltage and Energy Use

Figure 3.2 shows the reactor operational voltage and the energy use (in kWh/m^3) for both reactors. Results are given for i between 7.9 and 42 A/m^2 for RuO_2/IrO_2 and for i between 7.9 and 52 A/m^2 for Magneli.

The voltage increases with increasing i for both reactors. The RuO_2/IrO_2 shows a higher voltage for all tested i, and also a larger voltage increase per increase of i.
Due to the flow rate through the two reactors being the same, the energy use per unit of treated water follows the same trend as the voltage. At the chlorine plateau values indicated previously, the energy use per unit of treated water are 2.3 and 1.6 kWh/m^3 for RuO_2/IrO_2 and Magneli, respectively.

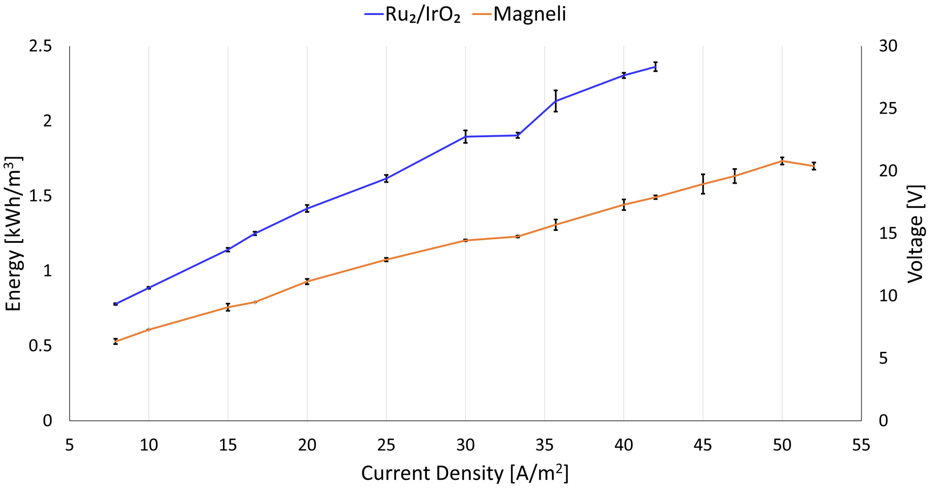

Figure 3.2: Voltage [V] and Energy use [kWh/m^3] in RuO_2/IrO_2 and Magneli reactors operating at constant q =300C/L and increasing i [A/m^2].

Fig 3.3 presents the energy use per unit of produced chlorine of the two reactors.

For both reactors, the energy per unit of produced chlorine decreases for increasing i, reaching at i =16.7 A/m^2 a stable value of 0.23 $kWh/g_{chlorine}$ for the RuO_2/IrO_2 and of 0.16 $kWh/g_{chlorine}$ for the Magneli.

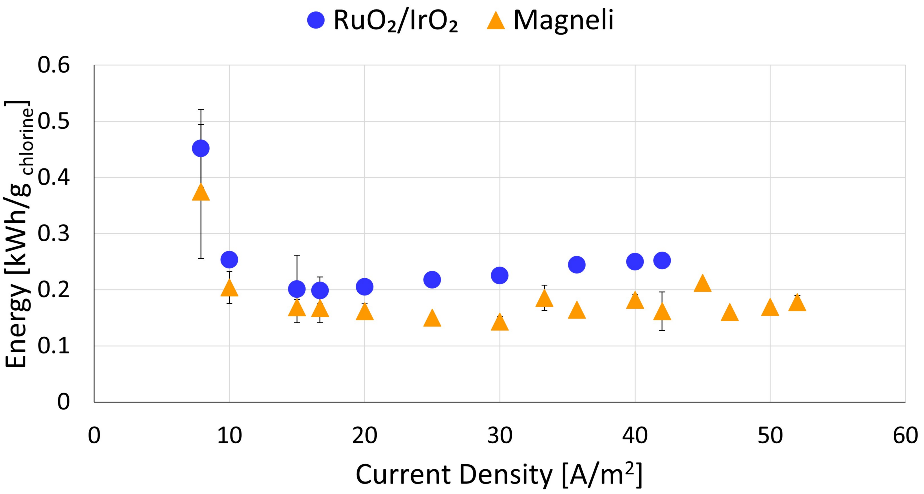

Figure 3.3: Energy use per gram of chlorine produced [kWh/m^3] for RuO_2/IrO_2 and Magneli reactors operating at constant q =300C/L and increasing i [A/m^2].

3.2. ED in the RuO_2/IrO_2 and Magneli reactors

This section presents the results for the disinfection experiments on the RuO_2/IrO_2 and Magneli operated for the four experimental settings described in Table 2.1.

3.2.1. Pathogen Removal overview

Figure 3.4 presents the *E. Coli* and ΦX174 removals expressed in logarithmic units for the experimental settings tested on the RuO_2/IrO_2 and the Magneli with the two electrolytes. The experimental data-points with an arrow (⬆), indicate that the pathogen count was below detection limit for both duplicates of the experiment. The triangle (▲) indicates that the pathogen count was below detection limit only for one of the duplicates.
For both pathogens, the removal increases for increasing q and i. The experiments mentioned in this chapter refer to the settings in Table 2.1.

Graph 3.4a shows the *E. Coli* removal in the RuO_2/IrO_2. When Na_2SO_4 is used as electrolyte, a LRV of 0.3 is observed for E1, whilst the LRV was below 0.1 for E2 and E3. It should be noted that the standard deviation of the removal at E1 was very high. When NaCl is used as electrolyte, the LRV achieved is above 5.0 for all tested settings. No CFU were observed in the duplicate of E2 for the chosen detection range.
Graph 3.4b shows the *E. Coli* removal in the Magneli. For Na_2SO_4 as electrolyte, a LRV below 0.1 is recorded for E1 and E2. At E3, a LRV of 0.6 is measured. For NaCl as electrolyte, a LRV of 4.5 is measured for E1. Doubling the q (E2, E3), no CFU were detected in the water, making the LRV higher than the maximum detectable for this experiment (LRV > 5.0).

For the experiments on ΦX174, PFU measurements were not conducted for experiment ϕ_1 by Na_2SO_4 because of the low removal observed for this setting by NaCl experiments.
Graph 3.4c shows the ΦX174 removal in the RuO_2/IrO_2. For all settings with Na_2SO_4 as electrolyte, the LRV was less than 0.1. For NaCl as electrolyte, a LRV of 0.2, 0.8, 1.2 was observed for ϕ_1, ϕ_2, ϕ_3 respectively. For ϕ_4, a LRV of 5.9 is observed in one experiment, and no PFU observed in the duplicate.
Graph 3.4d shows the ΦX174 removal in the Magneli. For Na_2SO_4 as electrolyte, a removal below 0.1 is observed for ϕ_2, ϕ_3, whilst a LRV of 0.9 is measured for ϕ_4. For NaCl as electrolyte, a faster removal is observed in the Magneli for increasing settings as compared to the RuO_2/IrO_2, with a measured LRV of 0.3, 2.5, 5.1 and 5.6 for ϕ_1, ϕ_2, ϕ_3, ϕ_4. In ϕ_4, no PFU is observed for either duplicate.

Overall, all removals obtained for RuO_2/IrO_2 operated with Na_2SO_4 as electrolyte were below 0.1, with the exception of E1 which was characterised by a large standard deviation. In the Magneli, the disinfection effect of non-chlorine species yields some results for q =600 C/L, but these results are also characterised by large standards deviations.

For all the tested experimental settings and for both reactors, the chlorine-based disinfection is the prevailing mechanism in the removal of both pathogens.

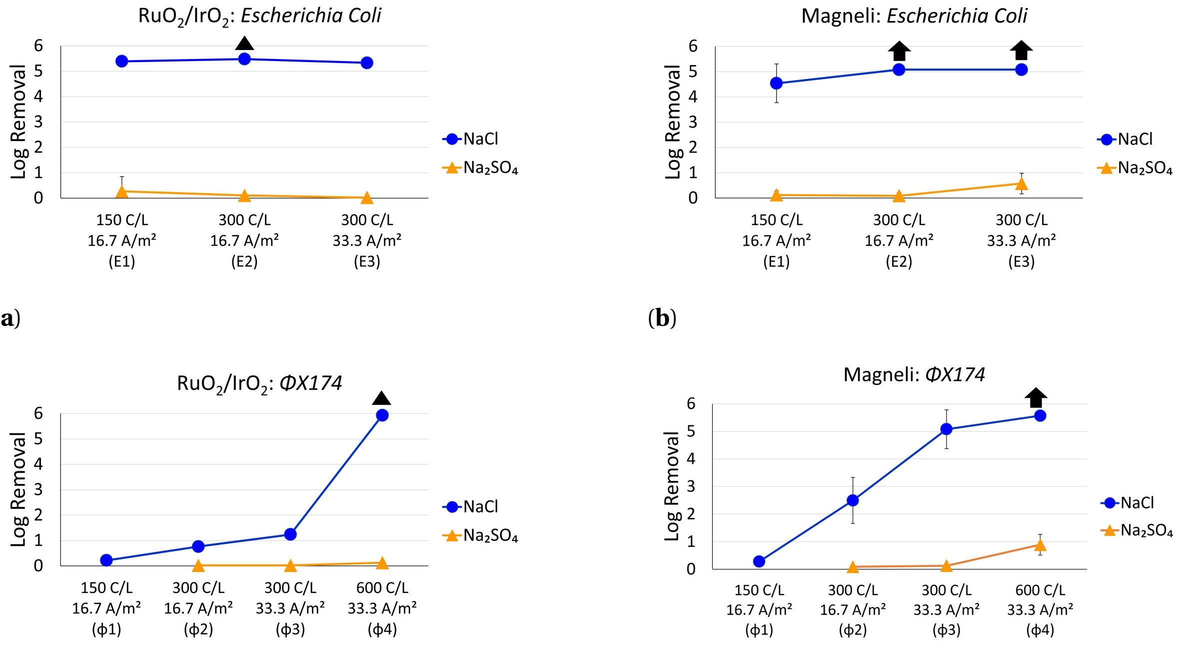

(**a**) (**b**)

(**c**) (**d**)

Figure 3.4: Overview of pathogen removal in log units for all disinfection experiments conducted on both reactors.

3.2.2. Trend of the pH throughout disinfection

Figure 3.5 shows the anodic pH measured at the end of each experiment, as well as the pH of the influent water. For all tested settings, the influent pH was 8.4.

The pH of the RuO_2/IrO_2 appears stable at constant q, with the exception on the experiments conducted at ϕ_4. At q =150 C/L and 300 C/L, the pH measures 6.8 and 6.3 respectively for both experiments on *E. Coli* and for ΦX174 with NaCl as electrolyte. For the experiment on ΦX174 with Na_2SO_4, the measured pH is 6.4 and 5.9 respectively for the two charge dosages. At ϕ_4, the measured pH decreases to 5.7 for NaCl electrolyte and to 3.5 for Na_2SO_4 electrolyte.
A stable pH trend cannot be observed for the Magneli, except at q =150 C/L where the pH is between 6.1 and 6.5 for all tested settings. Doubling the q at the same i determines an increase of the pH to around 7.0 for the *E. Coli* and Na_2SO_4 experiment, whilst the same electrolyte with ΦX174 decreases to below 4.0. The NaCl electrolyte shows an equal decrease for both pathogens to around 5.0. Doubling the i at constant q has a minor effect on the experiments with Na_2SO_4 as electrolyte, whilst the NaCl experiments show opposite trend, with the pH of the *E. Coli* experiment increasing to 6 and the ΦX174 decreasing to 4. Lastly, doubling the q once again to 600 C/L at brings the pH of the ΦX174 experiments with both electrolytes to 3.
Overall, the experiment conducted with ΦX174 and NA_2SO_4 as electrolyte shows the lowest pH trend for both reactors.

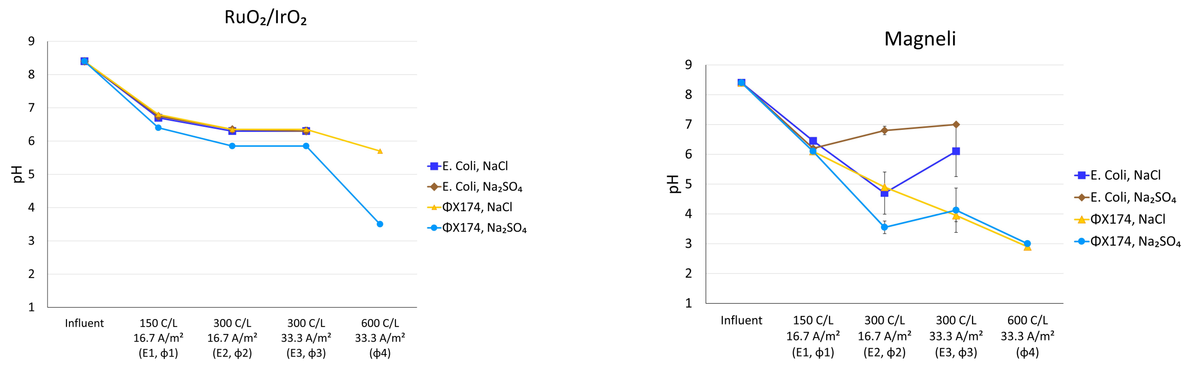

(a) **(b)**

Figure 3.5: pH trend observed for both reactors during the disinfection experiments.

3.2.3. Chlorine dose and residual for chlorine-based disinfection experiments

The measured chlorine dose and chlorine residual are presented in Figures 3.6 for *E. Coli* and 3.7 for ΦX174. Significant values for the chlorine residual are also highlighted.

The chlorine dose produced by the Magneli is higher than the RuO_2/IrO_2 for all tested settings. However, the difference in chlorine dose is small for q =150 and 300 C/L, whilst a large difference is observed at q =600 C/L for the Magneli (21.8 mg/L) and the RuO_2/IrO_2 (12.4 mg/L).

In the *E. Coli* experiments, the chlorine residual measured for all experiments is higher than the minimum chlorine residual required for distribution (0.2 mg/L).

A larger chlorine consumption is observed in the ΦX174 experiments, due to the higher initial concentration of the pathogen. For ϕ_1, ϕ_2, ϕ_3, the chlorine residual of the RuO_2/IrO_2 is 0 for all three settings, whilst it is respectively 0, 0.6 and 1.4 mg/L for the Magneli. In experiment ϕ_4, the large difference in produced chlorine dose reflects in chlorine residual measured for RuO_2/IrO_2 (0.2 mg/L) and Magneli (5.9 mg/L).

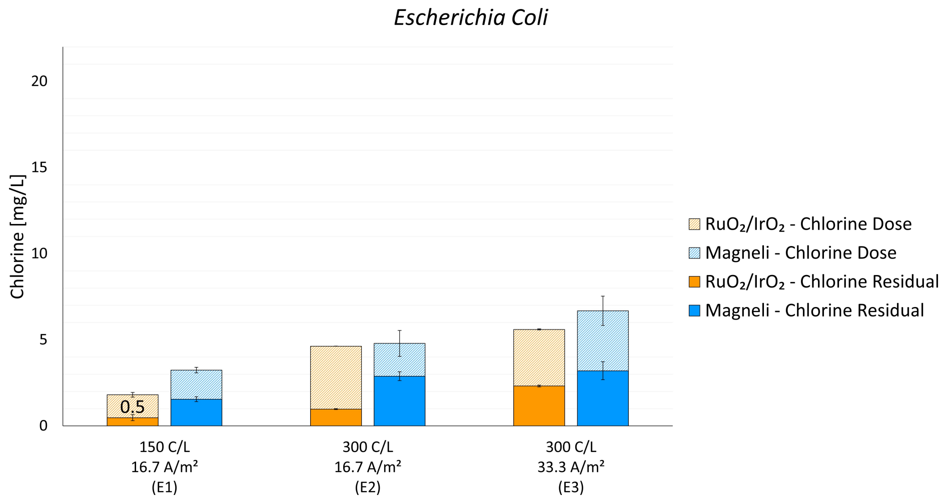

Figure 3.6: Chlorine Dose and Residuals for RuO_2/IrO_2 and Magneli reactors for experiments on *Escherichia Coli*. Significant values for residual chlorine are highlighted.

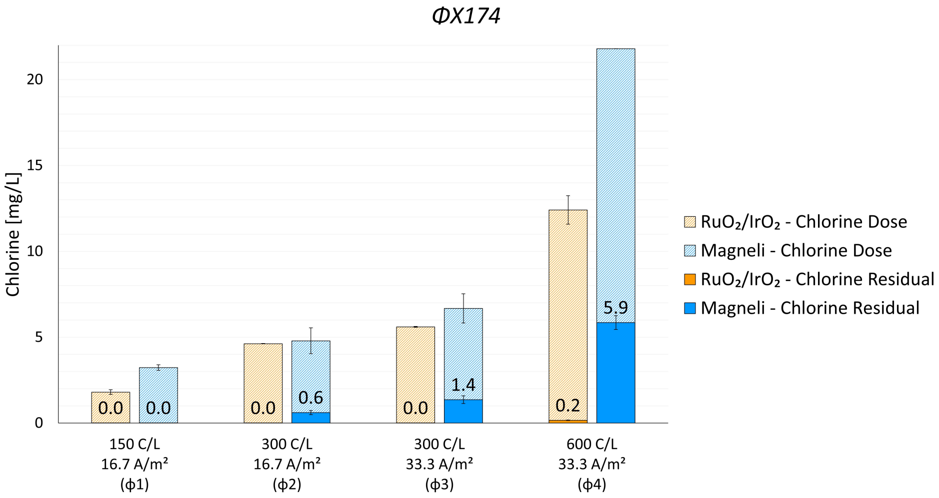

Figure 3.7: Chlorine Dose and Residuals for RuO_2/IrO_2 and Magneli reactors for experiments on ΦX174. Significant values for residual chlorine are highlighted.

3.2.4. Energy consumption for acquired log removal

Figures 3.8 and 3.9 show the energy use (in kWh/m^3) in each reactor to acquire a desired LRV of *E. Coli* and ΦX174 respectively. Experiments that resulted in no LRV are excluded from these graphs.

For experiments conducted using Na_2SO_4 as electrolyte, the highest removal achieved by the Magneli was 0.6 LRV for *E. Coli* and 0.9 for ΦX174 for energy consumptions of 0.63 and 2.71 kWh/m^3 respectively. The RuO_2/IrO_2 achieved limited removals of 0.3 (*E. Coli*) and 0.1 (ΦX174) for energy consumptions of 0.44 and 4.06 kWh/m^3 respectively.
With regards to chlorine-based disinfection, an *E. Coli* removal of at least 5 LRV is achieved for 0.41 kWh/m^3 for RuO_2/IrO_2 (LRV=5.4) and for 0.69 kWh/m^3 for Magneli (complete removal achieved, LRV>5.1). The Magneli also achieved at 0.31 kWh/m^3 a LRV of 4.5 for *E. Coli*. For ΦX174 removal by chlorine, a gradual increase in the LRV for increasing energy consumption can be observed for both reactors. The observed LRV in the Magneli increases faster for more moderate increases in energy consumption than in the RuO_2/IrO_2. To achieve a LRV of 5, an energy use of 2.88 kWh/m^3 for RuO_2/IrO_2 (LRV=5.9) and of 1.18 kWh/m^3 for Magneli (LRV=5.1) is required.

Overall, the Magneli shows a lower energy requirement to achieve a comparable LRV for both pathogens.

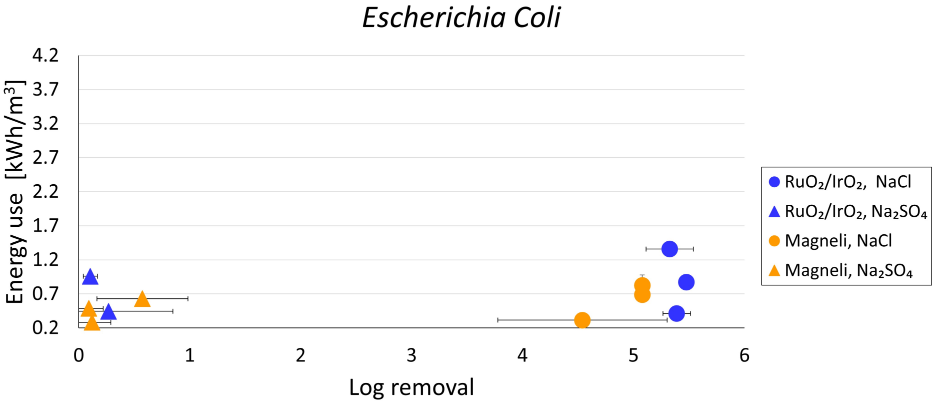

Figure 3.8: Energy use for required log removal for experiments conducted on *Escherichia Coli* for NaCl and Na_2SO_4 electrolytes on both reactors.

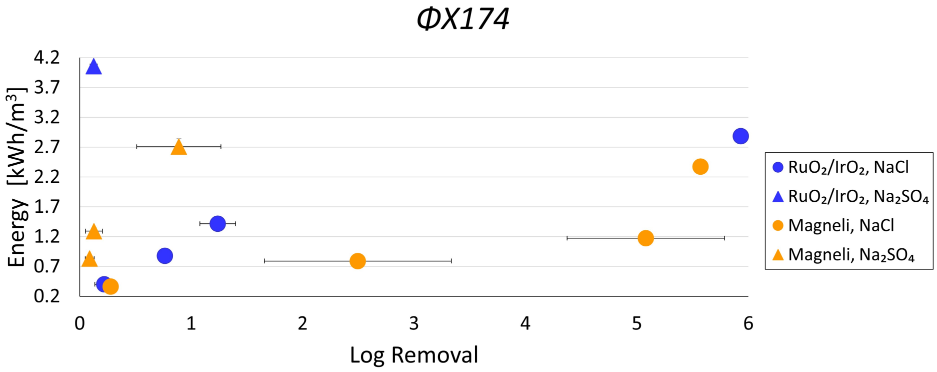

Figure 3.9: Energy use for required log removal for experiments conducted on ΦX174 for NaCl and Na_2SO_4 electrolytes on both reactors.

An overview of the disinfection experiments and the main measurements and findings is provided in summary Table 4.2 in Chapter 4.

3.3. RuO_2/IrO_2 performance in a field setting

Preliminary analysis on the collected waters showed that all the water types were of saline type (Electrical Conductivity (EC) > 10 ms/cm) therefore inadequate for direct human consumption (EC < 1 ms/cm). In particular, analysis on the sample collected from the Densu River showed an unexpectedly high EC for a river water (river water EC ia usually below 1 mS/cm). The water sample was collected from the Densu Delta estuary, so saline water infiltration from the surrounding lagoons and salt pans could be the reason for the high water conductivity. The turbidity of the seawater was below measurement range. Lastly, the pathogenic levels on all water types were too low to conduct complete analysis on the disinfection capacity of the reactor on real water sources.

Electrochemical experiments were performed on the water sources for constant q =300 C/L and increasing i [A/m^2]. The higher electrical conductivity of the water sources allowed to conduct experiments at higher i than those tested in the TU Delft laboratory, so the i was varied between 5 and 120 A/m^2 for seawater and between 10 and 120 A/m^2 for lagoon and river water.

3.3.1. Chlorine produced by electrochemical oxidation of different water sources

Figure 3.10 shows the chlorine production in the different water sources for constant q and increasing i.

For all water sources, the chlorine production increases for increasing i, reaching a plateau at i =20, 30 and 40 A/m^2, for seawater, lagoon water and river water respectively. The chlorine production reached a plateau of 35 mg/L for seawater and 5 mg/L for both river and lagoon water.

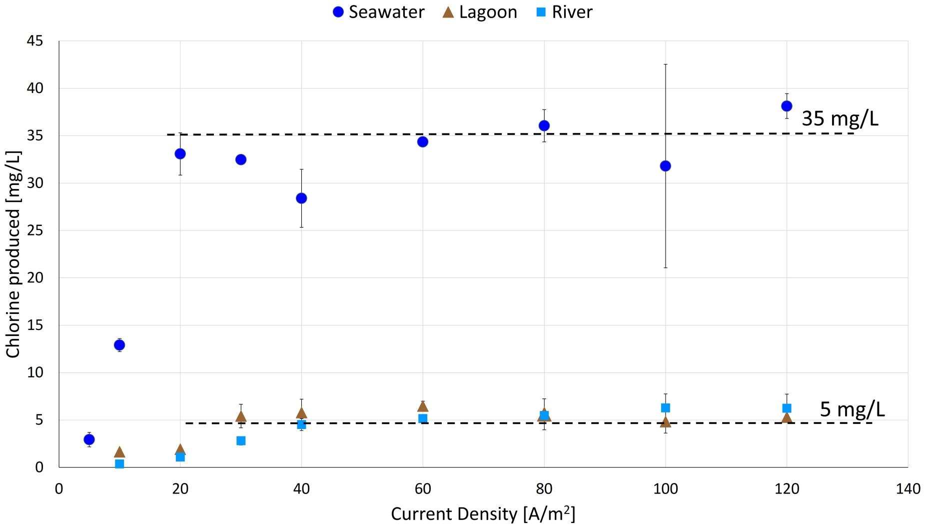

Figure 3.10: Chlorine production using different water sources in RuO_2/IrO_2 at q =300C/L and increasing i [A/m^2].

3.3.2. Voltage and energy consumption to produce chlorine from different water sources

Figure 3.11 presents the voltage trend for electrochemical oxidation with the RuO_2/IrO_2 on different water sources and for increasing i [A/m^2].

The cell voltage increases with increasing i, following an almost identical trend for seawater and lagoon water. The voltage of the river water has similar values at lower i, and starting from i =40 A/m^2 it shows a larger increase for increasing i.

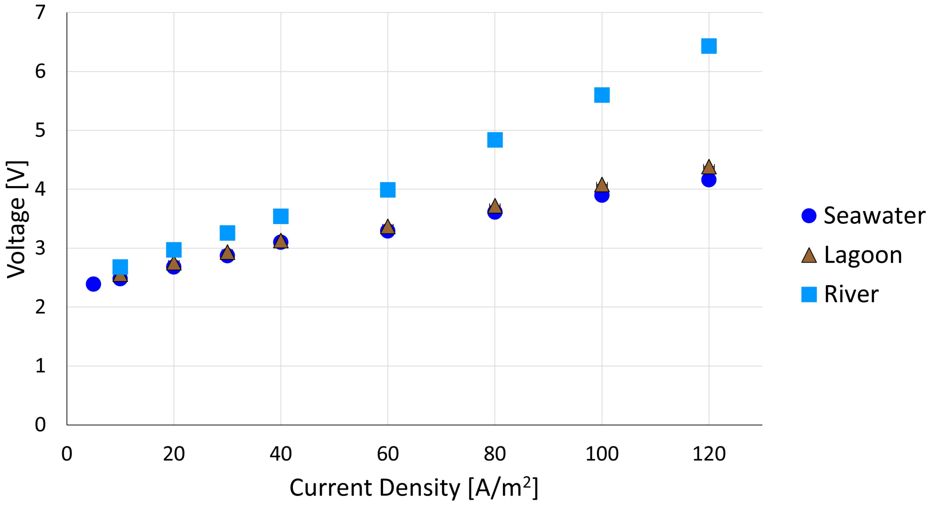

Figure 3.11: Voltage trend for electrochemical oxidation on different water sources at q=300C/L and increasing i [A/m^2].

Figure 3.12 shows the energy required to produce different chlorine doses from the three water sources.

The lagoon and the seawater show a similar energy requirement per unit of treated water. The river water shows similar energy use, but the energy requirements increase more rapidly than the other water sources, in line with what is observed in Figure 3.11. An effluent water containing 5 mg/L of free chlorine was produced with an energy use of 0.25 and 0.35 kWh/m^3 from lagoon and river water respectively. For the same energy consumption, an effluent water containing 32 and 38 mg/L chlorine was produced from seawater oxidation.

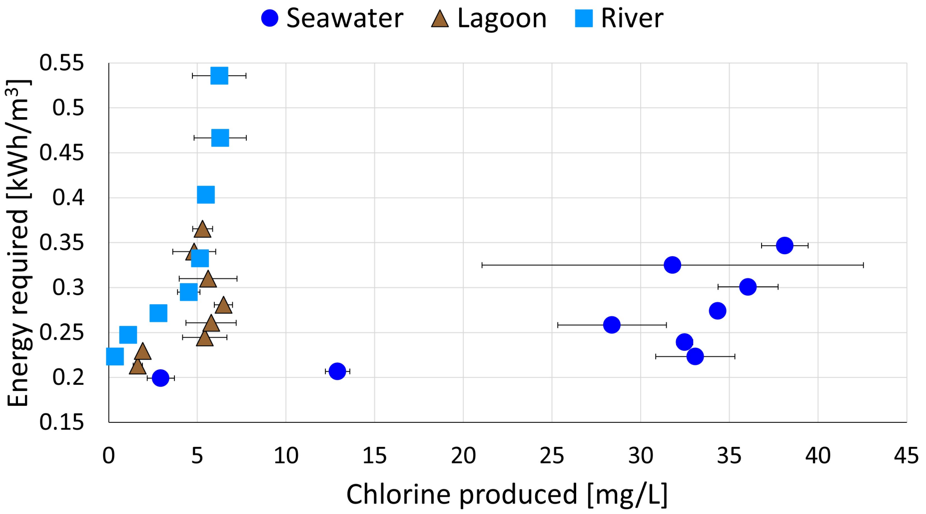

Figure 3.12: Energy required to produce desired chlorine dose in different water sources.

Figure 3.13 presents the energy use for increasing operational i , to produce a gram of chlorine for each water source. Values at i =10 and 20 A/m^2 for river water (corresponding to energy use of 0.94 and 0.23 $kWh/g_{chlorine}$) are not shown in the graph. The energy use for gram of chlorine produced decreases for increasing i , as chlorine production increases, and reaches a minimum at i =20 A/m^2 (0.007 kWh/m^3) for seawater and i =60 A/m^2 for lagoon (0.043 kWh/mm^3) and river water (0.065 kWh/m^3). It then increases slightly due to the increasing i .

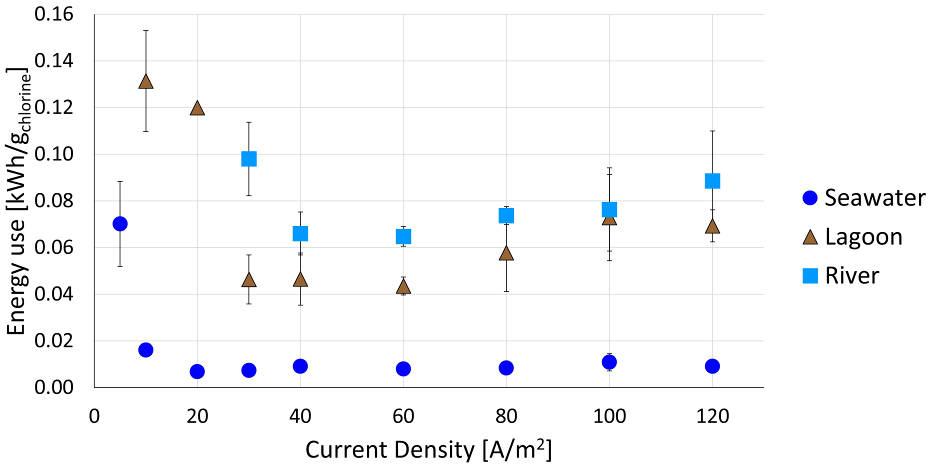

Figure 3.13: Energy use per gram of chlorine produced for applied i $[A/m^2]$.

An overview of the electrochemical chlorine production experiments on different water sources in Ghana, the main measurements and findings is provided in summary Table 4.3 in Chapter 4.

4

Discussions

In this chapter, the results relative to the laboratory and field experiments are explained. In the first section, the performance of the two reactors in producing chlorine when using a synthetic water matrix is discussed. The second section evaluates the results relative to electrochemical disinfection and how the two reactors performed according to the WHO standards. In the third section, the field results of the RuO_2/IrO_2 are analysed. The final section reflects on how the electrochemical results obtained in this research compare to traditional disinfection methods.

4.1. Performance comparison of RuO_2/IrO_2 and Magneli

Figure 3.1 underlines an almost comparable chlorine production performance for the two reactors. A substantial amount of literature agrees that active electrodes demonstrate higher chlorine production performances compared to non-active electrodes [48]. According to both Ghasemian et al. (2017) [28] and Jeong et al. (2009) [36], active DSA® type electrodes such as RuO_2/IrO_2 exhibit a higher chlorine production efficiency than the non-active BDD anodes, The same trend was not observed for this research.

The gradual increase in chlorine production observed at low i for constant q for both anodes is due to the chloride transfer through the inert anode and the effect of mass transfer limitations. At low i, low flow rates are kept to ensure the constant charge dosage q. This determines a low flow turbulence through the flow-through reactor and an increased boundary layer thickness which lowers the contact between dissolved chloride ions and the anode surface. As the i increases, the flow rate increases proportionally, decreasing the boundary layer and the mass transfer limitations. As a result, the chlorine production increases. At higher current densities, the flow rate increases and the HRT of the water in the system decreases. This could determine limitations in the conversion of chlorine, if the contact time is insufficient to ensure chloride oxidation to occur. When comparing the chlorine production of the RuO_2/IrO_2 and the Magneli, it must be kept in account that the two reactors where characterised by the same active anode surface and flow rate but different chamber volume, with the Magneli being smaller as described in chapter 2.1. As such, the comparisons between the performances of the two reactors cannot be completely equivalent, since for the same applied q, i and flow Q[L/s], the HRT in the Magneli will be smaller, signifying less contact time, as described in equation 2.2. In contrast, the smaller reactor chamber promotes increased contact between the water flow and dissolved chloride ions and the anode. Excluding the contribution of the anode material, the chloride oxidation performance of the two reactors becomes an assessment of which factor, between contact frequency (prevailing in Magneli) and chlorine conversion rate (prevailing in RuO_2/IrO_2), primarily affects the chlorine production.

4.1.1. Faradaic efficiency

From equation 2.3, the maximum free chlorine (as hypochlorous acid, HOCl, MW=52.46 g/mol) calculated for a supplied q =300 C/L is 81.3 mg/L. From the chlorine plateau values obtained for the two reactors, a Faradaic efficiency of 11.3% and 12.5% is observed for the CER in the RuO_2/IrO_2 and the Magneli respectively. The Faradaic efficiency is an indication of the propensity of an electrochemical reactor to produce a specific reaction, amongst all those happening in the electrochemical cell. When multiple (Faradaic) reactions are occurring in an electrochemical cell, the sum of their efficiencies should equal 100%. For the water matrix used for the experiments shown in 3.1, the two main reactions occurring in the anodic chamber are the CER (equation 1.2) and the OER (equation 4.1).

$$2H_2O \rightarrow O_2(g) + 4H^+ + 4e^- \quad E^0 = 1.23\,V \tag{4.1}$$

The similar standard electrode potential of the concurring reactions (1.23V for the OER and 1.36V for the CER) leads to competition in the occurrence of the two reactions, with the OER being thermodynamically favoured. The Faradaic efficiency indicates the portion of charge that is used for each reaction, and as such is an important factor to consider when wanting to enhance the CER [115]. The results show a clear selectivity for the OER in both reactors, for the influent water used. No significant difference in selectivity is observed between the RuO_2/IrO_2 and the Magneli, despite literature agreeing that competition between OER and CER tends to be more pronounced in active electrodes due to their low OER overpotential. Žeradjanin et al. (2014) observed that a higher CER selectivity is observed for increasing chloride concentrations, with an observed Faradaic efficiency of 97% for influent chloride concentrations of 10^5mg/L [115]. Therefore, the low CER selectivity and associated low Faradaic efficiencies for both reactors may be associated to the low chloride concentrations in the influent (50 mg/L).

4.1.2. Voltage and energy consumption

The voltage trend of the two reactors shows a clear increase in the operational voltage of the RuO_2/IrO_2 for the same operational conditions. As the applied i is equivalent for the two reactors for each experimental setting, this trend suggests a higher system resistance R in the RuO_2/IrO_2, according to equation 2.5. The electrochemical resistance in a cell depends on a number of factors, including anodic resistance, cathodic resistance, resistance across the cation exchange membrane and resistance in the solution media [94]. The RuO_2/IrO_2 cell had previously been used for other research, including reduction of metals [94] and oxidation of arsenic [83]. Furthermore, it was being used for PFAs oxidation in parallel to the disinfection experiments conducted in this research. Although the cell was cleaned from scaling and the membrane and cathode were changed regularly, the continuous operation may have caused polarization, and thus increased resistance, over time. Other factors involved in the cell resistance that are of interest for this research are the mass transfer limitations and the electrode overpotentials [66]. The mass transfer limitations directly influence the solution resistance, and solutions with homogeneously distributed ions that can diffuse to the anode present lower solution resistance [66]. Therefore it can be assumed that the increased contact between the flow and the anode in the Magneli reactor may impact in decreasing the solution resistance, and the higher mass transport rates observed in the Magneli by *Trellu et al. (2018)* may further contribute to this outcome [97]. The RuO_2/IrO_2 energy use observed at chlorine plateau value is higher than the energy per unit volume observed in previous electrochemical experiments conducted on this reactor: 0.45 kWh/m^3 for metal reduction, 0.066 kWh/m^3 in electrochemical advanced oxidation processes, 0.030 kWh/m^3 in horizontal embedded Fe-electrocoagulation, and 0.006 kWh/m^3 in Fe-electrocoagulation [94] [83] [43]. The q used was notably higher than the one used in these experiments (between 3 and 14 times higher than the q used for chlorine experiments in Rijsdijk 2022 [83], and contributes to the high energy values observed. This q was chosen with the aim of achieving large chlorine productions to balance the chlorine losses which would be expected due to turbidity and other factors in the field experiments. The high q, coupled to the low solution conductivity, determines high solution resistance and associated high energy consumptions, and from the field experiments results in Figure 3.12 it can be seen how energy consumptions per unit water decrease significantly when water electrical conductivity increases. In the scenario of implementing ED on a water with low conductivity, spiking the influent with NaCl to decrease the energy cost and boost chlorine production could be a solution and is proposed by Esposto (2009) [25] as a more affordable option than purchasing traditional chlorine products. In another study, a low chloride concentration of 50 mg/L (equivalent to the one used in this study) achieved a chlorine production of 2 mg/L with an energy consumption of 0.083 kWh/m^3. These experiments were performed in batch mode for a q =73 C/L applied over 50 minutes. The study also concluded that a chlorine dose of 4 mg/L could be achieved by dosing 110 mg/L chloride in the influent [85].

4.2. Electrochemical disinfection outcome

The graphs in Figure 3.4 show the clear predominance in the removal of both pathogens of the chlorine-based disinfection over the combined action of direct disinfection and ROS-based species.

For *E. Coli* disinfection by chlorine, the RuO_2/IrO_2 (Figure 3.4c) did not achieve the WHO safe water standard of 0 CFU/100 mL for either of the settings tested. The chlorine residual measured in the outflow (Figure 3.6) satisfies the minimum WHO requirement of 0.2 mg/L of chlorine to ensure safely stored household water treated by chlorination. Thus, further disinfection by chlorine can be expected outside of the reactor. In the Magneli (Figure 3.4b), the standard for safe drinking water is obtained for the settings at q =300 C/L, whilst the setting at q =150 C/L slightly under-performs (LRV < 5). Research shows that, at lower i , higher HRT are required to achieve higher disinfection efficiency, whilst at high i high inactivation efficiency is obtained regardless of contact time, anode surface area or chlorine concentration [50]. The lower HRT which characterises the Magneli may explain this slight underperformance. Furthermore, research shows that higher current densities may enhance water electrolysis and cause competition between the CER and the OER [50]. This phenomenon is expected to be more significant in an active anode, such as the RuO_2/IrO_2 because of the lower OER overpotential which characterises active anodes. This might explain the slight overperformance of the Magneli for the higher electrochemical settings. However, the smaller reactor chamber and higher chance of contact of the flow with the anode surface may also determine a more facilitated disinfection.

The performances of the two reactors in the removal of *E. Coli* and ΦX174 were evaluated by determining the standards reached by the electrochemical technology, according to the WHO standards for POU technologies [93]. For *E. Coli* disinfection by chlorine, the *highly protective* standard is successfully achieved by both reactors for all experimental settings (Figure 4.1). Thus, lower electrochemical settings can be used to obtain equivalent disinfection standards, saving on energy requirements (Figure 3.8).

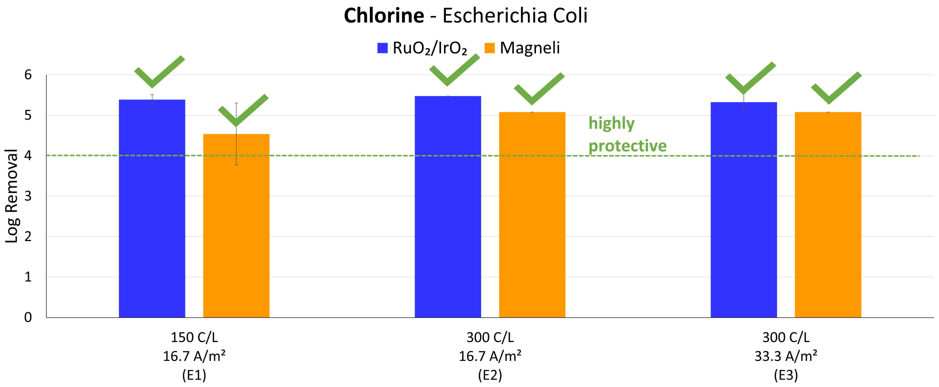

Figure 4.1: Electrochemical chlorine-based disinfection performance for *E. Coli* removal according to WHO standards for POU technology.

ΦX174 disinfection by chlorine achieves *highly protective* standards for ϕ_4 for both reactors, and for ϕ_3 for Magneli. The *protective* standard is not achieved by any of the settings not achieving the *highly protective* standard either, as shown in Figure 4.2. Furthermore, settings ϕ_1 to ϕ_3 for RuO_2/IrO_2 fail to provide any residual chlorine (Figure 3.7), therefore these settings are unsatisfactory for ΦX174 disinfection by electrochemically generated chlorine. For Magneli at ϕ_2, a residual chlorine of 0.6 mg/L is obtained. Therefore, the unsatisfactory removal achieved inside the reactor can still be achieved outside the reactor. The residual chlorine obtained for Magneli in ϕ_4 is above the maximum value of 5 mg/L chlorine concentration for human consumption as recommended by the WHO, Doubt arose on whether the high removal achieved in the Magneli for ϕ_4 was because of the low pH (Figure 3.5b). Literature indicates that phage sensitivity to pH varies between different phages, with more resistant phages being unaffected by pH 3, but no direct information was found for ΦX174 [37] [24].

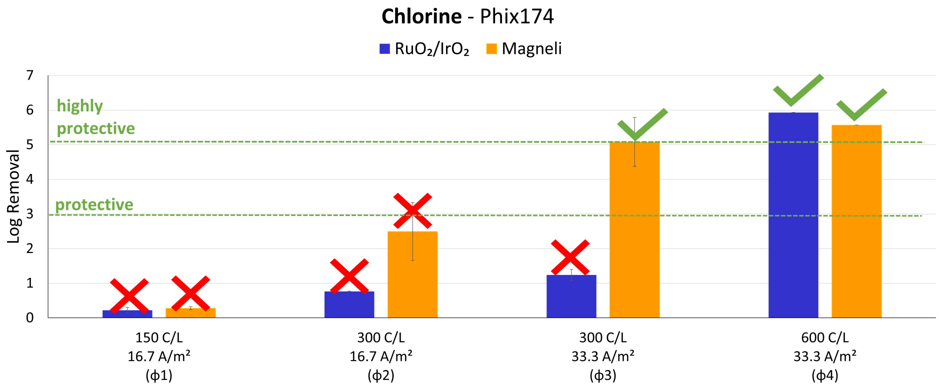

Figure 4.2: Electrochemical chlorine-based disinfection performance for ΦX174 removal according to WHO standards for POU technology.

Both *E. Coli* and ΦX174 disinfection by non-chlorine species (Figures 4.3 and 4.4) do not achieve the standards set by the WHO for POU technologies. Disinfection in absence of chlorine relies on the direct contact of pathogens via absorption on the anode surface, where the formed $OH^\bullet$ (ROS-based disinfection) is located or where the electron exchange (direct disinfection) occurs [80]. If the pathogen is not absorbed on the anode surface then disinfection occurs with difficulty. Ozone is an ROS formed via equation 1.8 which diffuses in the bulk of the solution, bypassing this limit. However, high potentials are needed to produce ozone, and as the $E_{\text{electrode}}$ was not measured it is not possible to know if the required potentials were reached. While sulphate ions were also present in solution, and sulphate oxidation has a lower E^0 than $OH^\bullet$ (2.44 V/SHE for sulphate as compared to 2.73 V/SHE for $OH^\bullet$), the results would not provide indication that sulphate radicals were formed. Nevertheless, the actual disinfection capacity of sulphate radicals is still unclear, and previous studies investigating the disinfection performance of sulphate radicals suggest that higher concentrations than those used in this research are needed to observe significant disinfection extent [105]. For what regards the effect of pH on the formation of ROS, no direct studies were found on the pH directly influencing $OH^\bullet$ formation, although an acidic pH would prompt the OER reaction as discussed in 4.2.1. A few studies on electrocoagulation agree that an acidic pH of 5.5 is favourable for the formation of ROS [11] and $OH^\bullet$ (pH 3) [29]. This might explain the slight increase in disinfection in experiment ϕ_4 for Magneli, but the same conclusion cannot be drawn for the increase in disinfection observed for Magneli in experiment E3.

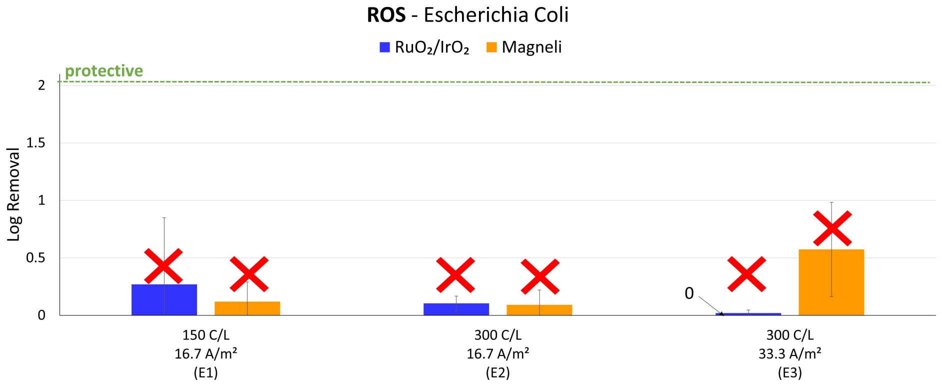

Figure 4.3: Electrochemical ROS-based disinfection performance for *E. Coli* removal according to WHO standards for POU technology.

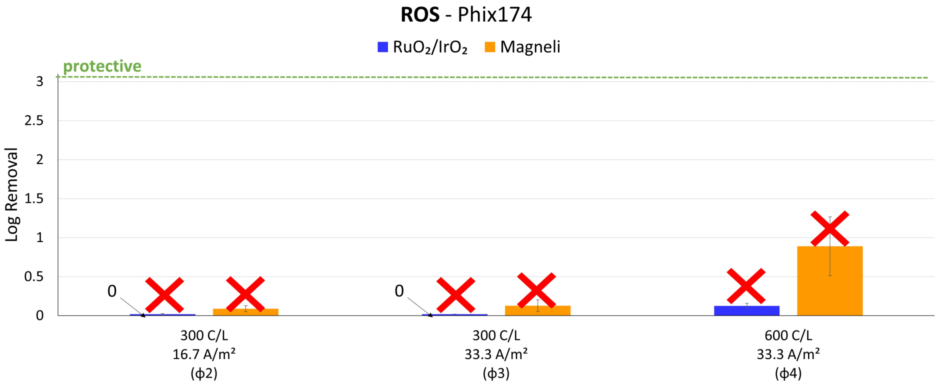

Figure 4.4: Electrochemical ROS-based disinfection performance for ΦX174 removal according to WHO standards for POU technology.

Overall, chlorine-based disinfection is prevailing in both reactors. The disinfection obtained in absence of chlorine species is deemed insufficient for disinfection standards, as described in graphs 4.3 and 4.4. This was an expected outcome for the RuO_2/IrO_2, but not for the Magneli, as extensive literature mentions the high capacity of Magneli-phase electrodes in producing $OH^\bullet$ species [27] [108] [107]. As discussed, the reasons behind the apparent absence of ROS disinfection observed in the Magneli cell could be connected to insufficient potential provided at the anode for ROS generation. ROS generation was observed in an experiment conducted by Jung et al. (2010) [38], using an influent with lower EC than in this study (250 μS/cm as compared to 400 μS/cm in this study). Similar i as this study were used (between 19.2 and 27 A/m^2) and the experiments were conducted in batch using a Pt/Ti electrode. Given that the $E_{\text{electrode}}$ is defined by the applied i, it may be assumed that the predominant factor in the limited ROS performance observed in the Magneli is the absence of interaction between surface generated $OH^\bullet$ and the pathogens. In another study using a flow-through reactor for the removal of *E. Coli*, ROS-mediated removal is achieved using i=58 A/m^2 and q=1200 C/L. which is two to eight times larger than the q used in this research [71]. Using higher q may prompt ROS production, but the scope of this research was to evaluate the portion of disinfection attributable to chlorine and to ROS in the two reactors, when using an influent water with characteristics resembling drinking water. Given that water sources used for human consumption will contain chloride, it can be concluded that for the settings applied chlorine-based disinfection is the prevailing mechanism for both reactors and independently achieves required water disinfection standards for both *E. Coli* and ΦX174.

In this research, for both electrolytes the RuO_2/IrO_2 and Magneli depict competitive disinfection capacities. Studies comparing the performance of different anodes types noted differing outcomes. Batch tests conducted by Rahmani et al. (2019) [80] observed that Pb/PbO_2 non-active anodes successfully oxidise organic compounds via the generation of $OH^\bullet$, but this efficiency is not reflected in bacterial removal. By contrast, the non-active SS/PbO_2 anode demonstrated higher efficiency than active anodes in ROS-based disinfection, while active anodes prevailed in removal of bacteria when NaCl was added to the system. The same author also underlined the greater disinfection power of electrochemically generated chlorine over ROS species, in both active and non-active anodes, and in general studies agree that ROS species intervene in ED when conditions are not favourable for the production of chlorine [48]. Dimensionally stable anodes (DSA®) such as RuO_2/IrO_2 demonstrated consisted reliability in chlorine production when chloride precursor is present and low oxidising capacities from the generated $OH^\bullet$ as compared to non-active electrodes [80]. Studies suggest that a lower electrode oxidising capacity ensures the stability of the electrogenerated chlorine, whereby anodes with high oxidising capacity such as Magneli and BDD may induce chlorine reaction with the formed $OH^\bullet$, forming the toxic chlorination byproducts chlorate and perchlorate. However, this effect was observed in batch reactors and over extended electrolysis periods, which does not apply to this research [104].

4.2.1. pH trend

The stable pH observed in the RuO_2/IrO_2 aligns with findings from previous research by Rijsdijk (2022) [83] using the same reactor, where the pH shows a steady trend for constant q. The lower pH observed in the Magneli may be the result of the lower HRT which hinders the H^+ diffusion through the membrane; however, uncertainties remain regarding its instability. The pH for water used for drinking water purposes should not be below 6.5, therefore pH adjustments are needed before using the water for consumption [68]. In general, ED cells that do not contain membranes separating the anodic and cathodic chambers have a neutral outflow pH [85]. However, a pH around 6 is favourable to maintain the produced dissolved chlorine in the form of HOCl. Furthermore, an acidic medium would also prompt the production of ROS as it favours the occurrence of the OER, which is required for the formation of $OH^\bullet$ via the intermediate reaction shown in equation 1.5. This is better observed in the Pourbaix diagrams (Figure 4.5) which show the thermodynamic equilibrium of the species in an electrochemical cell for varying pH. The diagram for water electrolysis (Figure 4.5a) is representative for ROS-based disinfection, and Figure 4.5b shows the water-chlorine solution which is representative for chlorine-based disinfection. With regards to water electrolysis and the potentials applied in an anodic cell, two reactions take place: the OER (equation 4.2) and the oxidation of hydroxide ions (OH^-) (equation 4.3). When water pH is basic, OH^- are present, which needs a lower supplied potential and will thus oxidise easier than the OER. In a water-chlorine solution, a slightly acidic pH above 3 ensures chlorine in the form of HOCl. Therefore, maintaining acidic pH in an anodic cell is preferential for both chlorine and ROS-based disinfection.

$$2\,H_2O\,(l) \longrightarrow O_2\,(g) + 4\,H^+\,(aq) + 4\,e^- \quad E^0 = 1.23\,V/SHE \tag{4.2}$$

$$4\,OH^- \longrightarrow O_2 + 2\,H_2O + 4\,e^- \quad E^0 = 0.401\,V/SHE \tag{4.3}$$

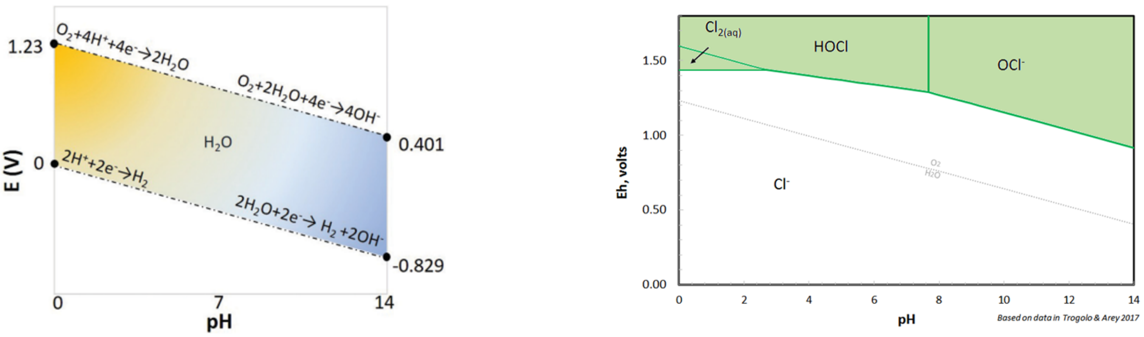

(a) Pourbaix diagram for water electrolysis. Reference: [9] [88]

(b) Pourbaix diagram for water-chlorine solution. Reference: [99] and designed by [2]

Figure 4.5: Pourbaix diagrams for different solutions.

An alternative solution to increase the effluent pH to acceptable values for drinking water (between 7 and 9.5) would be to bypass a portion of the anodic effluent to the cathodic cell, where the reduction reaction of water occurs (equation 4.4). This solution allows to keep the membrane and ensure a slightly acidic pH in the anodic cell, enhancing the disinfection process. Chlorine reduction can also occur in the cathodic cell (equation 4.5), which also provides a solution in the case that too much residual chlorine is produced at the anode [17]. Further considerations on the mechanisms of this process should be evaluated, such as the material of the cathode to ensure it doesn't corrode by chlorine and preventing scaling of reducing ions in the cathode chamber.

$$2\,H_2O + 2\,e^- \longrightarrow 2\,OH^- + H_2 \tag{4.4}$$

$$HOCl + H^+ + 2\,e^- \longrightarrow Cl^- + H_2O \quad E^\circ = 1.52\,V/SHE \tag{4.5}$$

4.2.2. Energy consumption in electrochemical disinfection

The energy consumption of the ED process in this study, when compared to other water treatment processes, is on the high end: with regards to other disinfection processes, UV disinfection consumes 0.05 kWh/m^3, ozone 0.1 kWh/m^3. Membrane processes are around 3 - 4 kWh/m^3, and some seawater reverse osmosis processes reach 2.6 kWh/m^3 [31],

The energy consumed in the system is directly correlated to the applied q and the system voltage according to equation 2.4. The q depends on the chosen operational settings, while the voltage is function of the applied i and system resistance (equation 2.5). To decrease the energy consumption in the electrochemical cell, the resistances have to be decreased. Three type of cell resistances can be defined: the ohmic (or electrolyte) resistance, discussed in section 4.1.2; the charge-transfer resistance, which defines the resistances of the electron transfer at the electrode-electrolyte interface and depends on the electrode and electrolyte type; and the diffusion resistance which is associated to the electrogenerated product concentrating on the electrode surface and is significant at high i where considerable product is being generated [69] [46]. The ohmic resistances are determined by the resistance encountered by the ions in travelling through the solution, associated with the electrolyte conductivity and with factors of cell geometry such as membrane and electrode thickness, membrane materials and distance between the electrodes. In this study, both electrochemical cells used contain a membrane, and the RuO_2/IrO_2 also contains spacers between the membrane and the electrodes which increases electrode spacing, which may also explain the larger resistances formed in the RuO_2/IrO_2 for the same influent.

Hand and Cusick (2021) [33] provide an overview of the energy consumed by different anode types tested in literature to achieve an LRV of 2 for *E. Coli* and of 3 for viruses. Both free chlorine and ROS as disinfectant are analysed, although for ROS-based disinfection only BDD, a class of non-active anodes extensively researched in literature, manage to achieve a 2 LRV for *E. Coli* for an energy consumption of 1 kWh/m^3. For chlorine-based disinfection, mixed metal oxides are shown to achieve 3 LRV for viruses at energy uses around 0.1 kWh/m^3, which is lower than the 0.79 kWh/m^3 measured to achieve a 2.5 LRV for ΦX174 in Magneli. However, specifications on the influent conductivity, as well as the electrochemical settings used are missing in Hand and Cusick's overview, therefore further conclusions cannot be made.

Norra et al. (2022) [71] conducted a ED experiment similar to the one in this research. *E. Coli* was spiked in real tap water containing low concentrations of chloride (21.4 mg/L) and sulphate (13.4 mg/L). This study used a one-time flow-through cell containing graphene-based sponge electrodes which had previously demonstrated high oxidation capacity for organic contaminants and simultaneously a very low chlorine current efficiency (0.04% in 10^3 mg/L NaCl), indicating that the main removal process occurring in this cell is not chlorine-mediated. An *E. Coli* removal of 5.5 LRV for an energy consumption of 5.70 kWh/m^3 for the chlorine-free system was obtained. From this research, the operational q and i required to achieve significant *E. Coli* removal without chlorine were 1200 C/L and 58 A/m^2 respectively.

4.3. Field performance

The variation in the RuO_2/IrO_2 performance for the CER when treating different water sources is discussed in this chapter.

Source	Water Type	Electrical Conductivity [mS/cm]	Turbidity [NTU]
Accra sea	Seawater	52.6	0[2]
Kpeshie Lagoon	Brackish Lagoon	26.7	37.42 (average)
Densu River	River	11.37	7.44 (average)

Table 4.1: Characteristics of water types collected in Ghana.

The main differences which affect the electrochemical performance and which characterise the water sources collected are the electroconductivity and the chloride content. The latter was not directly measured, but due to the seawater infiltration in the lagoon it can be assumed that the concentrations $[Cl^{-}{}_{sea}] > [Cl^{-}{}_{lagoon}] > [Cl^{-}{}_{river}]$. The direct effect of higher chloride contents, as compared to those tested in the TU Delft lab, is observed in Figure 3.10. As explained in chapter 4.1 and described by *Žeradjanin et al. (2014)*, the system selectivity for the CER increases when chloride increases in the influent [115], and for the maximum theoretical free chlorine concentration of 81.3 mg/L obtainable for a q =300 C/L, the Faradaic efficiencies measured for the three water sources at their plateau values are of 43.1% for seawater and 6.2% for lagoon and river water. When evaluating these results however, it should be considered that the turbidity present in the water may be consuming the produced chlorine before it can be measured, therefore the Faradaic efficiency of the system for the CER may actually be higher. The higher chloride concentrations also determine a decrease in the mass transfer limitations effect, with the plateau chloride value reached at lower applied i for increasing chloride concentrations.

4.3.1. Voltage and energy consumption

The effect of the different electrical conductivities is observed in the different operational voltages in Figure 3.11. The electrical conductivity measures the capacity of a solution to carry electrical current. Therefore, it impacts the solution (or ohmic) resistance in the cell and requires higher voltage to operate the reactor at the same i with less conductive water. This trend is observed when operating the reactor with river water. These observations provides insight into chlorine production using different water sources. Waters with higher electrical conductivity require less energy, as shown for the lagoon and sea water in Figure 3.12. Despite the seawater having double the conductivity of lagoon water, this does not affect the energy demands when operating the system using either water source. This suggests that, for the applied i, the lower conductivity of the lagoon still ensures sufficient conductivity for the current to flow without increasing system resistance. The same is observed for the river water when operated at lower i, but increasing i determines a rapid increase in resistance. Therefore, depending on the concentration of chlorine that wants to be achieved, different water types depending on local availability can be used with equivalent energy consumption. Given the high chlorine concentrations generated, seawater is a valid option to produce a concentrated chlorine solution which may be used for in-line chlorination units.

4.3.2. Chlorine production and water turbidity

Free chlorine is readily consumed by organic matter present in the water, and WHO standards for chlorine doses for disinfection are determined based on the level of turbidity of the water, as mentioned in Introduction 1.3.2 [51] [48] [56]. The observed turbidity (measured in NTU) was above desirable for chlorination experiments conducted on the lagoon and river water. The turbidity of the water prior to disinfection experiments should be below 1 NTU for effective disinfection, and when that is not possible the aim should be to keep the turbidity below 5 NTU. Above these values, chlorination can still be practiced but the chlorine dose required to guarantee pathogen inactivation increases significantly [75]. The measured turbidity in the water collected classified the samples as *clear water* for the river, and *turbid water* for the lagoon, according to WHO standards [74]. Despite higher electrical conductivity and possibly more chloride ions in the lagoon water due to seawater infiltration, the observed chlorine production was similar to that of the river. The turbidity and chlorine production were monitored throughout the experiments and shown in Figure 4.6. The

---

[2] Turbidity below instrument detection range

average turbidity measured over all experiments is shown. It should be noted that the measured turbidity associated with each chlorine measurements is the net turbidity after oxidation by the chlorine produced. Therefore, it is expected to decrease from the influent value. This trend is observed for the river water, but not for lagoon water. It's hypothesized that heavier organic particles became preponderant in the influent bottle as water was pumped into the reactor.

Issues associated with chlorine oxidation of organics are also the formation of DBPs, which is an important issue in drinking water due to the health effects on humans and has demonstrated the same formation potential as chemical chlorination when applying in-line electrolysis [51] [10] [14] [101]. Given the turbidity levels present in these waters, DBPs formation can be expected. Similarly to traditional disinfection, coupling ED with other water treatment steps (pre-treatment by electrocoagulation is one example) is a growing area of research in electrochemistry for water treatment [10] [48].

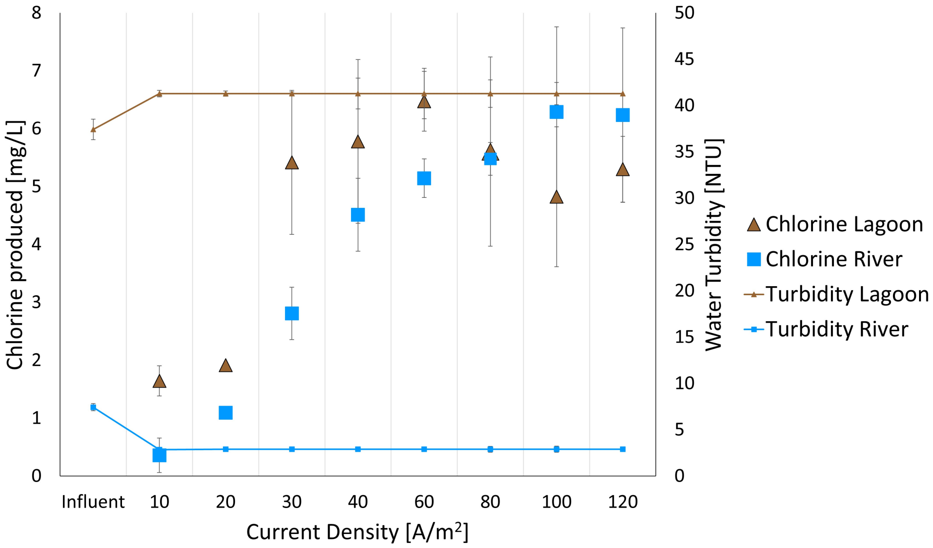

Figure 4.6: Electrochemical chlorine production from different water sources: effect of turbidity [NTU].

4.4. Electrochemical System compared to traditional disinfection

Global human health and progress is closely connected to access to safe drinking water, which is still lacking in areas that, for a number of reasons, cannot rely on traditional centralized treatment systems. Decentralized systems allow to bridge the gap by building small-scale infrastructure that relies on local water sources to achieve results comparable to centralized systems. Decentralized technologies significantly assist rural communities in accessing safe drinking water, as they can operate either on a community or household-scale to supplement unreliable or deficient water treatment lines. When implementing small-scale, local disinfection units, microbiological safety of the water has to be provided while ensuring low treatment costs. Furthermore, these units must be independent from the energy grid, and designed to be robust, reliable and user-friendly [71].

Adopting ED systems as alternative to traditional chlorination is a compelling option due to its autonomous operation, safe and easy usage, facility to adapt the setup to diverse settings, and low land usage. When adopting this novel technology in place of traditional disinfection, a number of considerations must be made.

Similarly to traditional disinfection, the performance is function of the influent characteristics, which in the case of ED also encompasses the chemical attributes (electrical conductivity and chloride content) of the water. When these are very low, the energy consumption and efficiency of the system rapidly change, owing to limited ion diffusion and significant ohmic losses attributable to the increased system resistance [48]. With a focus on Ghana, the main surface water sources of the country are rivers (the Volta River system, the South-Western River system and the Coastal River system) [110]. Rivers and lakes tend to have low conductivity levels, and tests conducted at different stations on the Volta basin measured EC as low as $63\,\mu S/cm$ [6]. Combined with water turbidity, which varies depending on the river flow, rains, seasonal factors (higher temperatures increase algae and plankton growth) and basin morphology, the performance of an ED cell can vary greatly. While altering the characteristics of the influent water (ie., by adding salt to increase the EC) may be troublesome and compromise the operational simplicity of the ED, it can be argued from the results of this study that turbidity is the primary factor hindering the chlorine production. Thus, operating on removing the turbidity, for example by adopting an electrocoagulation cell, could provide a comprehensive treatment system consisting of technologies using synergistic effects to meet field setting demands.

The main drawback associated to the use of electrochemical systems as compared to traditional disinfection are the high investment costs (Capital Expenditures (CAPEX)), especially related to the anode, and the operational costs to run the system (Operational Expenditures (OPEX)) [5] [96]. This research focuses primarily on the OPEX related to the energy use of the system, as calculated for the performed experiments, with the objective of comparing the costs in providing electrochemically produced chlorine to traditional chlorination.

Using river water, the RuO_2/IrO_2 shows an optimised energy use of 0.064 $kWh/g_{chlorine}$ corresponding to operational $i = 60\ A/m^2$ for the applied $q = 300\ C/L$. As of 2023, the price of electricity for Ghanaian households amounted to 1.65 Ghanaian cedi/kWh [95]. This corresponds to an OPEX of 0.11 Ghanaian cedi/$g_{chlorine}$, or 0.0073 €/$g_{chlorine}$. Literature indicates varying chlorine costs depending on the product type. Different products used for chlorination at POU are liquid and tabular chlorine, as well as flocculant-disinfectant [18]. The most commonly used chlorine tablets reported by Crider et al. (2023) for POU disinfection are the Aquatabs® brand, which deliver 5 mg/L chlorine to 20L of turbid water for an equivalent cost per unit chlorine of 0.3 €/$g_{chlorine}$ [8] [18]. Thus, the OPEX costs of using an electrochemical system to produce chlorine are 40 times cheaper than traditional chlorine tablets. Additional specific costs that affect chlorine tablets are delivery, transportation and staff costs [52]. However, the installation costs for chlorine tablets are basically zero [25]. As compared to chlorine gas, ED is an expensive option but bypasses the safety risks associated with transport and storage of chlorine gas tanks [25].

OPEX costs on the field can be mitigated by connecting the electrochemical cell to renewable energy sources, and powering these systems through the use of solar panels is a gaining significant attention in recent literature [33]. Photovoltaic is a valuable energy source in countries with high solar irradiation, and for sub-Saharan Africa this resource holds promising potential. According to results from the Solar and Wind Energy Resource Assessment (SWERA) Ghana Project report, Ghana receives sufficient sunlight to provide between 4 and 6 hours of useful solar energy per day. Assuming Ghana's solar power potential (irradiation received by the sun [kWh/surface area receiving the sun per day] x hours of sun) to be 4.5 kWh/m^2 and a commercial photovoltaic conversion efficiency of 15%, it is calculated that 1 m^2 solar panel can produce an estimated 0.68 kWh/d of electric energy in Ghana [87]. This would allow to produce, from the river water tested in this research, 2.1 m^3/day of treated water containing 5 mg/L chlorine. This could provide a small community of about 50 people assuming a water demand of 0.04 m^3/person/day [45]. When compared to the Aquatabs® tablets, which can provide 5 mg/L chlorine at the equivalent cost of 1.5 €/m^3 (24.3 Ghanaian cedi/m^3), opting for this alternative would results in savings of 50 Ghanaian cedi/day for the community. However, a significant implication of a system powered by solar panels is the discontinuous treatment cycle, which impacts both the continuous availability of treated water and the possible implications in operating an electrochemical system in on/off mode. A buffer system that can store treated water can mitigate the impacts of intermittent water supply. In this design, treated water is collected in a clean reservoir containing residual chlorine to prevent re-contamination. The chlorine in the reservoir should be monitored regularly and especially before water is consumed, to ascertain that it meets the minimum residual chlorine requirement of 0.2 mg/L, which ensures that all pathogens are removed.

The ED design could also be used to create an in-line system with the highly concentrated chlorine solution obtained from seawater electrolysis. In-line or passive chlorination, as opposed to manual household chlorination, is commonly done by water passing through slowly dissolving chlorine tablets which gradually release disinfectant agent, or by liquid chlorine dosers (Figure A8.1). Passive chlorinators are highly valued as they operate without energy and independently dose chlorine, outperforming manual household chlorination which relies on user adherence to dosing protocols. Limitations of traditional passive chlorinators include its reliance to chlorine availability and accessibility, which can be disrupted in the supply chain. Furthermore, the high cost of solid tablets and the variable quality of local liquid chlorine can pose challenges [52]. Dössegger et al. (2021) [23] estimated the cost of passive chlorinators providing 2 mg/L chlorine an average of 0.54 \$/m^3, or 8.1 Ghanaian cedi/m^3. These costs accounted for maintenance expenses, labor and chlorine refills, and correspond to 4 Ghanaian cedi/$g_{chlorine}$ provided. These would indicate much larger OPEX than electrochemically producing chlorine from seawater (energy use of 0.007 kWh/$g_{chlorine}$ corresponding to 0.012 cedi/$g_{chlorine}$, considering Ghanaian electricity prices). Further research on the implementation of this system would yield interesting insight.

The CAPEX remain the most significant contribute when adopting electrochemical systems, with the costs per surface (m^2) of the electrodes used in this research ranging between 2000-4000 € for RuO_2/IrO_2 and 4000-6000 € for Magneli. The cell type used in this experiment (flat-plate electrodes) is a more common design amongst RuO_2/IrO_2 and DSA® electrodes, while Magneli cells are more accessible in other design types.

Anode Type	Experiment Setting			Log Removal		**Chlorine Dose**/Residual [mg/L]			Effluent Anodic pH	Energy [kWh/m^3]	
		Charge Dosage [C/L]	Current Density [A/m^2]	Ecoli	Phix		Ecoli	Phix		Ecoli	Phix
RuO$_2$/IrO$_2$	E1, ϕ_1	150	16.7	5.4	0.2	**1.8**	0.5	0.0	6.7	0.41	0.40
	E2, ϕ_2	300	16.7	5.5▲	0.8	**4.6**	1.0	0.0	6.3	0.87	0.88
	E3, ϕ_3	300	33.3	5.3	1.2	**5.6**	2.3	0.0	6.3	1.36	1.42
	ϕ_4	600	33.3	-	5.9▲	**12.4**	-	0.2	5.7	-	2.88
Magneli	E1, ϕ_1	150	16.7	4.5	0.3	**3.2**	1.6	0.0	6.3	0.31	0.36
	E2, ϕ_2	300	16.7	5.1⬆	2.5	**4.8**	2.9	0.6	4.8	0.69	0.79
	E3, ϕ_3	300	33.3	5.1⬆	5.1	**6.7**	3.2	1.4	5.1 [3]	0.83	1.18
	ϕ_4	600	33.3	-	5.6⬆	**21.8**	-	5.9	3.0	-	2.36

Table 4.2: Summary Table of the disinfection experiments conducted and significant values. LRV with ⬆ indicate that the pathogen count was below detection limit for both duplicates of the experiment, while ▲ indicates that pathogen count was below detection limit for only one of the duplicates. Values for effluent anodic pH are averaged over *E. Coli* and ΦX174, and significant differences (when measured) are indicated.

Water Type	Current Density [A/m^2] at plateau chlorine	Chlorine Produced [mg/L]	Effluent Anodic pH	Energy [kWh/m^3]	Energy [kWh/g$_{chlorine}$]
Seawater	20	33	5.5	0.22	0.007
Brackish Lagoon	30	5.4	6.4	0.24	0.046
River	40	4.5	6.2	0.29	0.066

Table 4.3: Summary Table of chlorine production experiments performed on different water types collected in Ghana, at q =300 C/L.

---

[3] Anodic effluent pH measured 6.1 for *E. Coli* and 3.9 for ΦX174

5

Conclusions and Recommendations

5.1. Conclusions

The electrochemical reactors tested, an active RuO_2/IrO_2 and a non-active Magneli anode, showed successful chlorine production in low conductivity waters. The Faradaic efficiency measured for the chlorine production at q =300 C/L for the RuO_2/IrO_2 and Magneli was 11.3% and 12.5%, respectively. For the same current density (i), the operational voltage of the Magneli is lower than the RuO_2/IrO_2, reflecting lower system resistances and associated lower energy consumption. As the current density increased from 7.9 to 42 A/m^2, the difference in voltage increased from being 32% to 37% lower for the Magneli compared to the RuO_2/IrO_2. This determines slightly higher energy consumption to acquire a similar output for the RuO_2/IrO_2.

Both the RuO_2/IrO_2 and the Magneli demonstrated high bacteria (*E. Coli*) and virus (ΦX174) removal when performing chlorine-based ED, with the Magneli providing higher residual chlorine and, at q =600 C/L, also a higher initial chlorine dose. The anodic pH trend of the RuO_2/IrO_2 showed higher stability at a constant q, as compared to the Magneli. The WHO standard for POU technologies of *highly protective* disinfection technology for *E. Coli* was achieved by both reactors at q =150 C/L, i =16.7 A/m^2, corresponding to an energy use per unit of treated water of 0.41 and 0.31 kWh/m^3 for RuO_2/IrO_2 and Magneli respectively. For ΦX174, the standard was achieved at q =300 C/L, i =33.3 A/m^2 for Magneli (1.18 kWh/m^3), and at q =600 C/L, i =33.3 A/m^2 for RuO_2/IrO_2 (2.88 kWh/m^3). For ROS-based disinfection, the WHO standards were not reached for any of the tested settings, and the Magneli showed a slight removal of 0.6 for *E. Coli* at q =300 C/L, i =33.3 A/m^3 and 0.9 log for ΦX174 at q =600 C/L, i =33.3 A/m^3, which however corresponded to very high energy requirements for unsatisfactory log removals. In conclusion, the Magneli provided similar log removals for lower energy consumption, but a more unstable anodic pH trend.

In field experiments, electrochemically produced chlorine was successfully produced in waters with different characteristics. Highly concentrated chlorine solution for in-line chlorination is a possibility when performing electrochemical oxidation on seawater, where the high conductivity and high chloride content allow the generation of chlorine with low system resistances and associated low energy consumption (0.007 kWh/$g_{chlorine}$). In lower conductivity river water, for an energy use of 0.33 kWh/m^3 a dose of 5 mg/L chlorine was achieved, which was above the WHO standard of 4 mg/L chlorine for disinfection of turbid waters. Water turbidity was a limiting factor to the electrochemical chlorine production, and should be removed prior to the electrochemical system if the aim is to produce chlorine for disinfection.

Implementation of ED in decentralized settings proved to be a cost-competitive technology from an OPEX perspective when compared to POU disinfection using chlorine tablets, with the electrochemical system producing chlorine from river water at a cost that is 40 times cheaper than the equivalent dosage provided by chlorine tablets. While the OPEX are higher than using chlorine gas, it has important advantages when used for decentralized settings. It eliminates the need for transportation to restock chlorine product, thus bypassing the safety risks associated to transporting chlorine gas, and the extra costs for manpower and vehicle expenses. Additionally, transportation may be a challenge in decentralized settings very hard to reach. Lastly, the chlorine generated by ED systems tend to be of higher quality than both chlorine gas and tablets, due to the additional compounds present in the tablets and in the impurities which may form in gas tanks after long storage periods.

5.2. Recommendations

While the chlorine-based disinfection was well observed and easily comprehensible due to the possibility of performing chlorine measurements, which established that chloride oxidation was indeed occurring, understanding the functionality of the ROS-based disinfection was challenging. The short lifespan of ROS makes it challenging to measure their formation, making it unclear whether the absence of disinfection in ROS-based disinfection was due to experimental conditions being too low and/or water parameters being unfavourable to produce ROS, or if the pathogens were not successfully removed despite the formation of ROS. Performing additional experiments using an anode potentiostat would yield further information on the processes occurring in the anodic cells. In general, developing further understanding on the correlation between the applied i and $E_{\text{electrode}}$, particularly for the Magneli, would offer further insights on the different disinfection capabilities of the reactor.

The issues associated with high turbidity levels in ED source water for the conducted field experiments were mentioned. When implementing the ED step as post-chlorination, it is necessary to precede it with a turbidity removal process to enhance chlorine production and limit the formation of DBPs. Hand and Cusick (2021) [33] mention that hybrid technologies coupled with ED to fully treat different waters is a growing research field. The coupling of electrocoagulation and ED is a valid option to provide both turbidity reduction and disinfection treatment in decentralized treatments using technologies that operate similarly and can be powered by renewable energy sources.

In the context of using ED as a final disinfection step for drinking water use, the pH of the effluent anodic water has to be adjusted to fall within the acceptable range for human use (pH between 6.5 and 8.5) [68]. The reactors tested in this research contained a membrane which separated the anodic and cathodic cells. Removing the membrane would determine a more neutral outflow pH due to the mixing of the OH^- generated at the cathode and the H^+ generated at the anode, but keeping anodic pH around 6 maximises the chlorine present in HOCl form. Therefore, keeping the membrane to have greater control over the anodic pH and adjusting the effluent anodic pH accordingly is the preferred choice. An alternative set-up which can be evaluated is bypassing a portion of the anodic effluent to the cathodic cell.

The sensitivity of electrochemical systems to varying water compositions was observed in this study, but the waters tested were characterised by a high chloride content. Some freshwater sources such as rivers, which are viable supplies for ED, contain lower chloride content than those used in this study (less than 1 mg/L). Evaluating the variation in disinfection processes and energy requirement when using freshwater of different compositions is a viable continuation of this study. Furthermore, this study did not evaluate the removal efficiency on real water sources, which would provide insight on how the system compares with common disinfection methods used on the field.

Conducting an in-depth CAPEX evaluation and correlating the findings with traditional disinfection technologies used in decentralized settings would determine the competitivity of the system with already available methods. Lastly, evaluating the feasibility and implications of operating the system on solar panels would help in providing a concrete idea of the implications and benefits of applying the technology to decentralized environments.

Appendix

A1. Pump curves

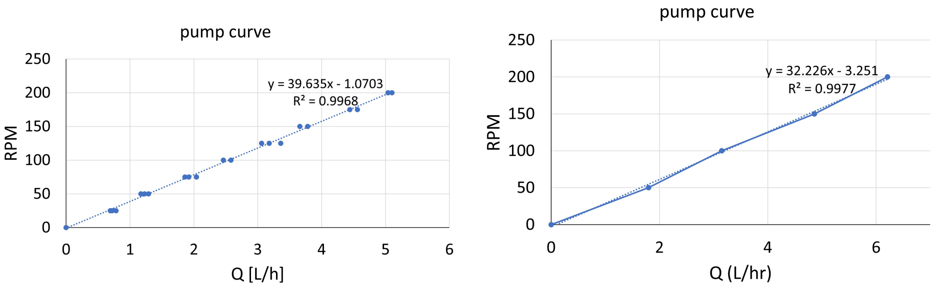

(a) RuO$_2$/IrO$_2$ pump curve

(b) Magneli pump curve

Figure A1.1: Electrochemical reactors pump curves

A2. Chlorine phases and pH

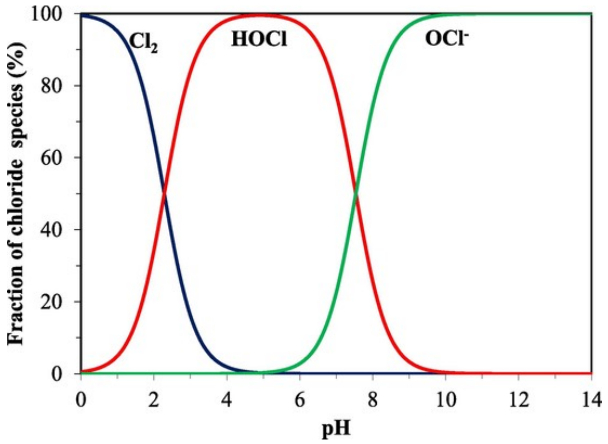

Figure A2.1: Chlorine species distribution in solution as function of pH, at standard temperature and pressure, Luna-Trujillo et al. (2020) [55]

.

A3. Anode Materials: Literature overview

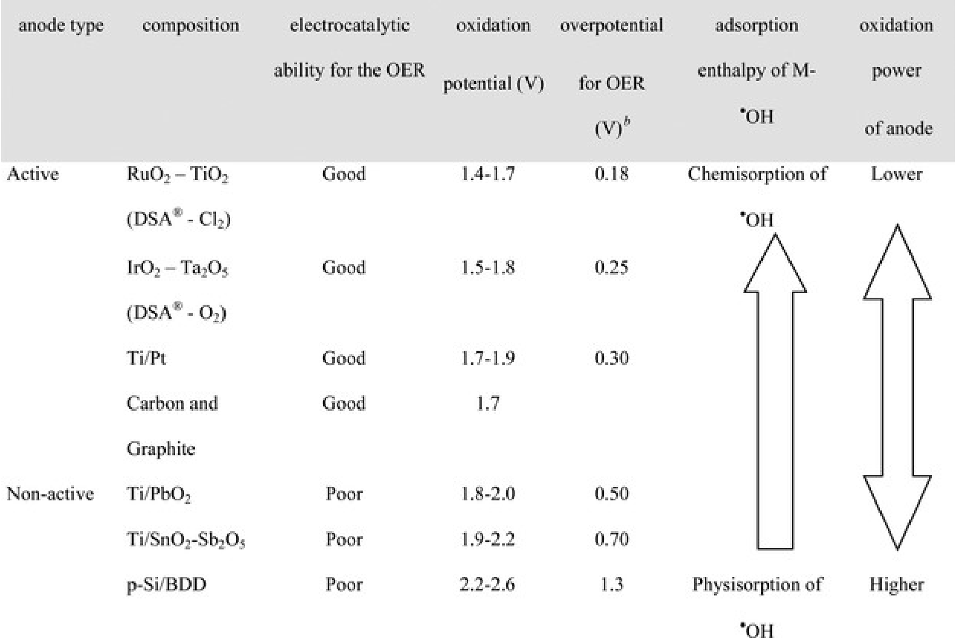

anode type	composition	electrocatalytic ability for the OER	oxidation potential (V)	overpotential for OER (V)^b	adsorption enthalpy of M-•OH	oxidation power of anode
Active	$RuO_2 - TiO_2$ (DSA® - Cl_2)	Good	1.4-1.7	0.18	Chemisorption of •OH	Lower
	$IrO_2 - Ta_2O_5$ (DSA® - O_2)	Good	1.5-1.8	0.25		
	Ti/Pt	Good	1.7-1.9	0.30		
	Carbon and Graphite	Good	1.7			
Non-active	Ti/PbO_2	Poor	1.8-2.0	0.50		
	Ti/SnO_2-Sb_2O_5	Poor	1.9-2.2	0.70		
	p-Si/BDD	Poor	2.2-2.6	1.3	Physisorption of •OH	Higher

Figure A3.1: Anode Materials and properties with regard to the OER. Reference: Martínez-Huitle et al. (2015) [59]

.

A4. Chlorine production experiments

Charge Dosage [C/L]	Current Density [A/m^2]	HRT$_{RuIr}$ (min)	HRT$_{Magneli}$ (min)
300	4	25	12
300	7.9	12.7	6
300	10	10	4.8
300	15	6.7	3.2
300	16.7	6	2.8
300	20	5	2.4
300	25	4	1.9
300	30	3.3	1.6
300	35.7	2.8	1.3
300	40	2.5	1.2
300	42	2.4	1.1
300	25	2.2	1.1
300	47	2.1	1
300	50	2	1
300	55	1.8	0.9

Table A4.1: Chlorine production: Experimental settings

A4.1. Chlorine measurements for HRT 3 and HRT 30’

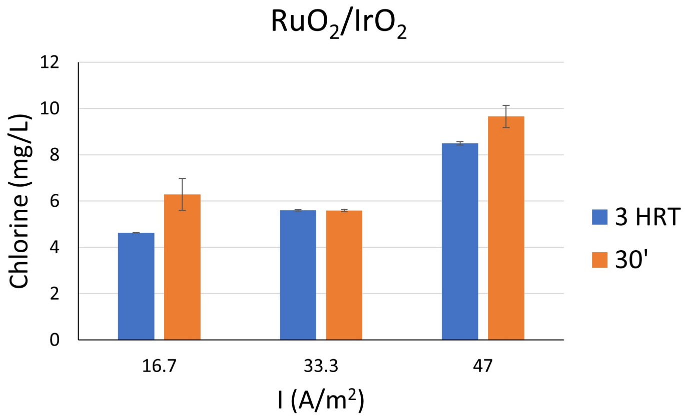

Figure A4.1: RuO_2/IrO_2 chlorine production for two sampling times. Fixed CD=300 C/L

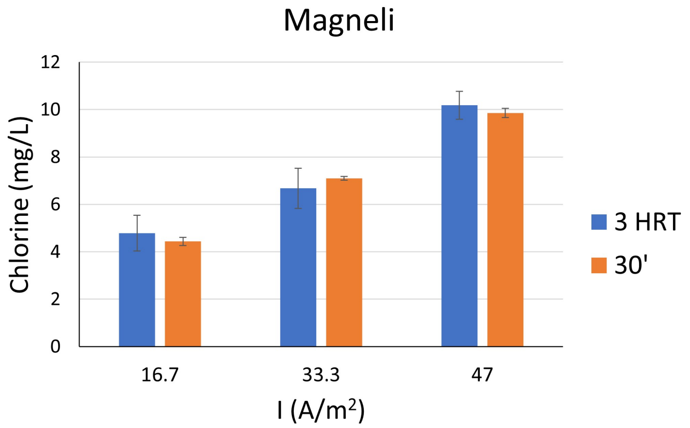

Figure A4.2: Magneli chlorine production for two sampling times. Fixed CD=300 C/L

A5. Electrochemical Disinfection Experiments

A5.1. ED: experimental data points

Setting E.coli	Setting Phix	q [C/L]	i [A/m^2]	HRT$_{RuIr}$ (min)	HRT$_{Magneli}$ (min)
E1	ϕ_1	150	16.7	3	1.5
E2	ϕ_2	300	16.7	6	3
E3	ϕ_3	300	33.3	3	1.5
-	ϕ_4	600	33.3	6	3

Table A5.1: ED: Experimental settings

A5.2. RuO_2/IrO_2 counts

	NaCl			Na2SO4		
	DR	Sample Vol (mL)	Counts	DR	Sample Vol (mL)	Counts
Influent	100	0.1	3	100	0.1	8
Influent	100	0.1	3	100	0.1	13
Influent	10	0.1	8	-	-	-
Influent	10	0.1	11	-	-	-
E1	1	50	1	100	0.1	23
E1	1	100	1	10	0.1	60
E2	1	50	0	10	0.1	22
E2	1	100	2	100	0.1	9
E2	1	100	0	10	0.1	59
E2	1	100	1	100	0.1	7
E3	1	100	1	10	0.1	113
E3	1	100	2	100	0.1	12
E3	-	-	-	100	0.1	11
E3	-	-	-	10	0.1	»
E3	-	-	-	10	0.1	»

Table A5.2: RuO_2/IrO_2 counts for disinfection experiments of *E. Coli*

	NaCl			Na2SO4		
	DR	Sample Vol (mL)	Counts	DR	Sample Vol (mL)	counts
Influent	10000	1	100	10000	1	39
Influent	10000	1	71	10000	1	37
Φ1	10000	1	45	-	-	-
Φ1	10000	1	59	-	-	-
Φ2	1000	1	149	10000	1	49
Φ2	1000	1	145	10000	1	48
Φ3	1000	1	38	10000	1	54
Φ3	1000	1	64	-	-	-
Φ4	1	1	1	10000	1	30
Φ4	1	1	0	10000	1	27

Table A5.3: RuO_2/IrO_2 counts for disinfection experiments of ΦX174

A5.3. Magneli counts

	NaCl			Na2SO4		
	DR	Sample Vol (mL)	Counts	DR	Sample Vol (mL)	counts
Influent	10	0.1	8	100	0.1	38
Influent	10	0.1	16	100	0.1	35
E1	1	50	6	100	0.1	21
E1	1	50	0	-	-	-
E1	1	100	2	100	0.1	41
E2	1	100	0	100	0.1	40
E2	1	100	0	100	0.1	24
E3	1	100	0	100	0.1	5
E3	1	100	0	100	0.1	19

Table A5.4: Magneli counts for disinfection experiments of *E. Coli*

	NaCl			Na2SO4		
	DR	Sample Vol (mL)	Counts	DR	Sample Vol (mL)	counts
Influent	10000	1	48	10000	1	34
Influent	10000	1	58	10000	1	42
Influent	10000	1	30	-	-	-
$\phi1$	10000	1	30	-	-	-
$\phi1$	10000	1	26	-	-	-
$\phi2$	1000	1	5	10000	1	33
$\phi2$	100	1	45	10000	1	29
$\phi2$	100	1	3	-	-	-
$\phi2$	10	1	32	-	-	-
$\phi3$	1	1	1	10000	1	32
$\phi3$	1	1	10	10000	1	25
$\phi4$	1	1	0	10000	1	10
$\phi4$	1	1	0	1000	1	81
$\phi4$	-	-	-	10000	1	2
$\phi4$	-	-	-	1000	1	33

Table A5.5: Magneli counts for disinfection experiments of ΦX174

A5.4. ORP graphs

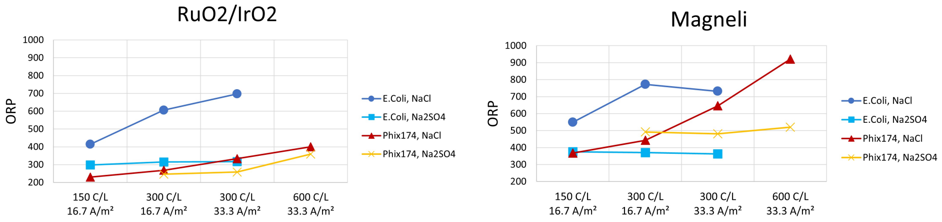

(a) RuO$_2$/IrO$_2$ ORP trend **(b)** Magneli ORP trend

Figure A5.1: ORP trend during electrochemical disinfection

A5.5. Voltage trend

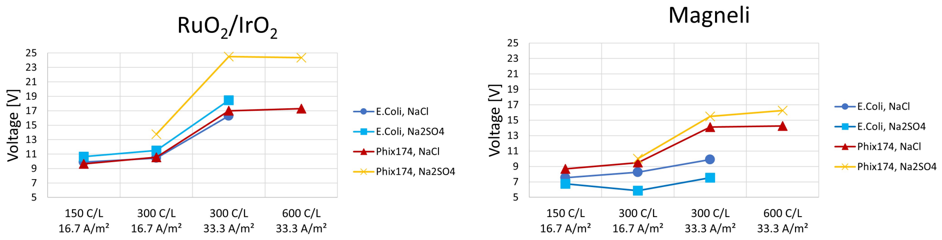

(a) RuO$_2$/IrO$_2$ Voltage trend **(b)** Magneli Voltage trend

Figure A5.2: Voltage trend during electrochemical disinfection

A6. Disinfectant properties of different oxidants

A6.1. Free chlorine

The release of atomic oxygen (equations) determine the disinfecting effect of free chlorine [44].

$$\mathrm{HClO} \rightleftharpoons \mathrm{O} + \mathrm{Cl}^- + \mathrm{H}^+ \tag{A6.1}$$

$$\mathrm{ClO}^- \rightleftharpoons \mathrm{O} + \mathrm{Cl}^- \tag{A6.2}$$

A6.2. Sulphate

Sulphate (SO_{42}^{-}) undergoes anodic oxidation forming peroxodisulphate ($S_2O_8^{2-}$) (equation A6.3, an oxidant species which can then decompose to sulphate radicals ROS (equation A6.4):

$$\mathrm{SO_4^{2-}} \rightarrow \mathrm{S_2O_8^{2-}} + 2e^- \quad E^0 = 2.44\,\mathrm{V/SHE} \tag{A6.3}$$

$$\mathrm{S_2O_8}^{2-} \longrightarrow 2\,\mathrm{SO_4}^{\bullet} \tag{A6.4}$$

A6.3. Other ROS

Hydrogen peroxide (H_2O_2) (Equation A6.5) and ozone (O_3) (Equation A6.6) are commonly mentioned ROS in literature [7]:

$$2\,\mathrm{H_2O} \longrightarrow \mathrm{H_2O_2} + 2\,\mathrm{H}^+ + 2\,\mathrm{e}^- \quad E^0 = 1.78\,\mathrm{V/SHE} \tag{A6.5}$$

$$\mathrm{H_2O} + \mathrm{O_2} \longrightarrow \mathrm{O_3} + 2\,\mathrm{H}^+ + 2\,\mathrm{e}^- \quad E^0 = 2.07\,\mathrm{V/SHE} \tag{A6.6}$$

A6.4. Intermediates of the OER

The overall OER is given as follows:

$$2\mathrm{H_2O}(l) \rightarrow \mathrm{O_2}(g) + 4\mathrm{H}^+(aq) + 4\mathrm{e}^- \quad E^0 = 1.23\,\mathrm{V/SHE} \tag{A6.7}$$

Comninellis (1994) described the mechanism of formation of ROS via the OER intermediates forming at the anode surface (M), distinguishing between the process occurring in active anode types and the process occurring in non-active anode types [15].

$$\mathrm{M} + \mathrm{H_2O} \rightarrow \mathrm{M(OH^{\cdot})} + \mathrm{H}^+ + \mathrm{e}^- \tag{A6.8}$$

For both anode types, the first step is the oxidation of water on the anode (M) surface to form adsorbed hydroxyl radicals $M(\mathrm{OH}^{\cdot})$ (*physically adsorbed active oxygen*) (Reaction A6.8):

From here, the stronger interactions of the $OH^{\bullet}$ with the electrode surface in active anodes will prompt the formation of the higher metal oxide (MO) (*chemically adsorbed active oxygen*) (Reaction A6.9).
The chemisorbed active oxygen will then oxidize substances present on the anode surface; however, it competes with the side reaction of the OER due to the chemical decomposition of the higher oxide (Reaction A6.10).

$$M(\mathrm{OH}^{\cdot}) \rightarrow \mathrm{MO} + \mathrm{H}^+ + \mathrm{e}^- \tag{A6.9}$$

$$\mathrm{MO} \rightarrow \mathrm{M} + \frac{1}{2}\mathrm{O_2} \tag{A6.10}$$

On the other hand, the weak interactions between the $OH^{\bullet}$and the non-active anode surface will determine the direct action of the physisorbed $OH^{\bullet}$in oxidising substances on the anode surface. Xie et al. (2022) discusses that the physisorbed $OH^{\bullet}$ desorbs and interacts as solvated $OH^{\bullet}$ with the contaminants in solution Equation A6.11)[108].

$$M(\mathrm{OH}^{\cdot}) \rightarrow M + \mathrm{OH}^{\cdot} \tag{A6.11}$$

This reaction is in competition with the side reaction of hydroxyl radicals oxidation (Reaction A6.12) [58].

$$M(\mathrm{OH}^{\cdot}) \rightarrow M + \frac{1}{2}O_2 + \mathrm{H}^+ + \mathrm{e}^- \tag{A6.12}$$

From the $\mathrm{OH}^\bullet$formed, other ROS are formed as described in equations 1.6 to 1.8 A diagram of the full process of the OER is given in Figure A6.1:

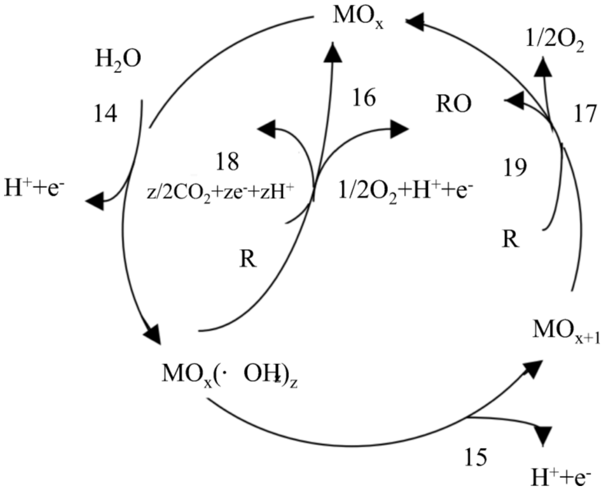

Figure A6.1: Comninellis (1994) ROS formation via intermediates of the OER diagram, where R represents the organics being oxidised [15]

A7. Field Experiments

A7.1. Experimental data points

Charge Dosage [C/L]	Current Density [A/m^2]	HRT$_{\text{RuIr}}$ (min)
300	5	20
300	10	10
300	20	5
300	30	3
300	40	2.5
300	60	1.5
300	80	1.3
300	100	1
300	120	0.5

Table A7.1: Field experiments: Experimental settings

A7.2. WHO standards for POU technologies

Target	Log$_{10}$ reduction required: bacteria	Log$_{10}$ reduction required: Viruses
Highly Protective	≥ 4	≥ 5
Protective	≥ 2	≥ 3

Table A7.2: WHO disinfection standards for viruses and bacteria for POU technologies

A7.3. Characteristics collected water samples

Source	Water Type	Electrical Conductivity [mS/cm]	Turbidity [NTU]
Accra sea	Seawater	52.6	0
Kpeshie Lagoon	Brackish Lagoon	26.7	37.42 (average)
Densu River	River	11.37	7.44 (average)

Table A7.3: Characteristics of collected water types

A7.4. ORP

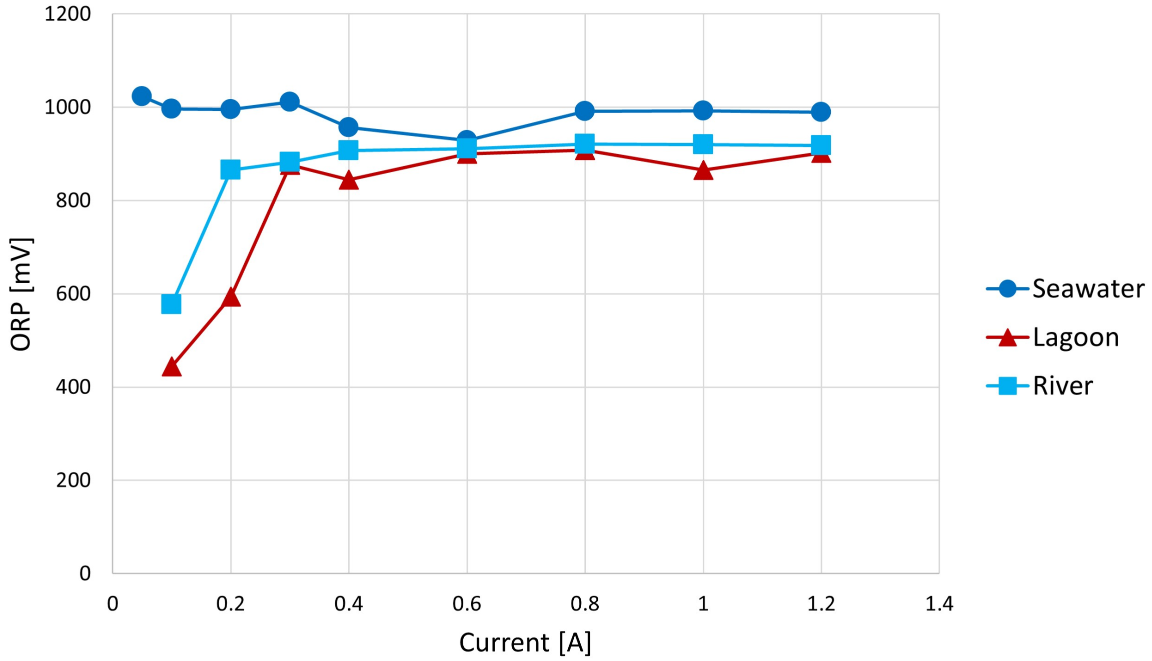

Figure A7.1: ORP for the three water types

A7.5. Voltage

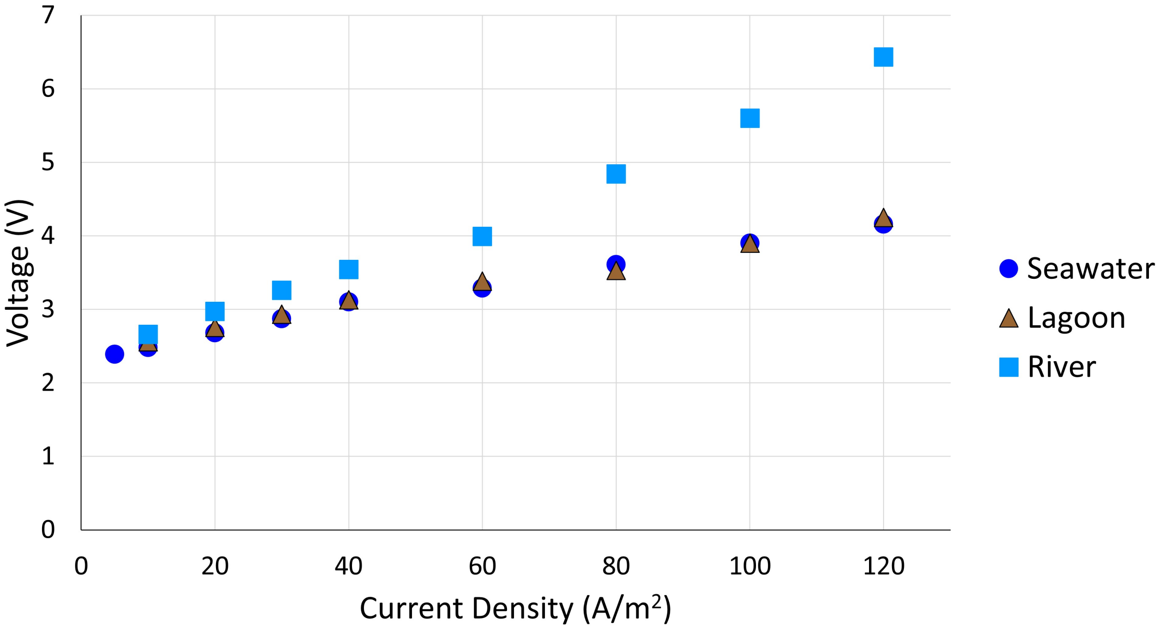

Figure A7.2: Voltage for increasing Current Density for three water types tested on the RuO_2/IrO_2

A7.6. Trend of the pH for the different water sources during electrochemical oxidation

The pH trend for increasing i, as well as the influent pH of each water source, is presented in Figure A7.3:

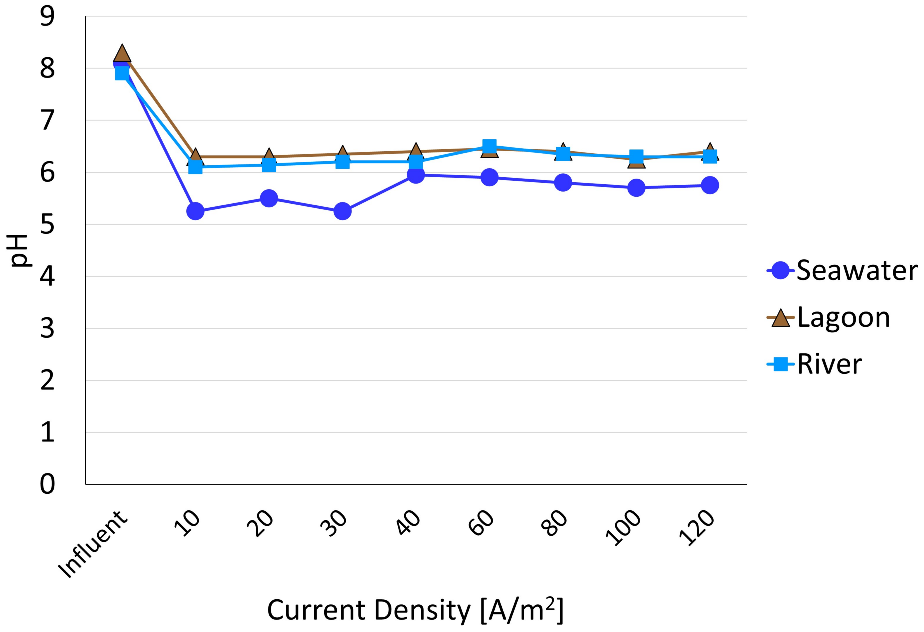

Figure A7.3: pH trend for electrochemical oxidation on different water sources at CD=300C/L and increasing current density i (A/m^2)

The three water sources show a stable pH trend for constant q and increasing i.
The pH of all three influents is around 8. For the lagoon and river water, the pH decreases to 6 from i =10 A/m^2, and remains stable for all experiments. In the seawater, the pH initially decreases to 3.7 at i = 5 A/m^2 (data point not shown in graph), then increases to 5.25 for i between 10 and 30 A/m^2. It then remains stable at around 6 for i between 40 and 120 A/m^2.

A8. Passive chlorination

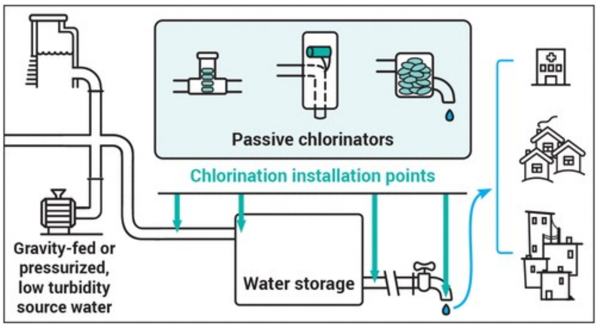

Figure A8.1: Traditional in-line chlorination examples, taken from: Lindmark et al. (2022) [52]

A9. Pictures of the Set-ups

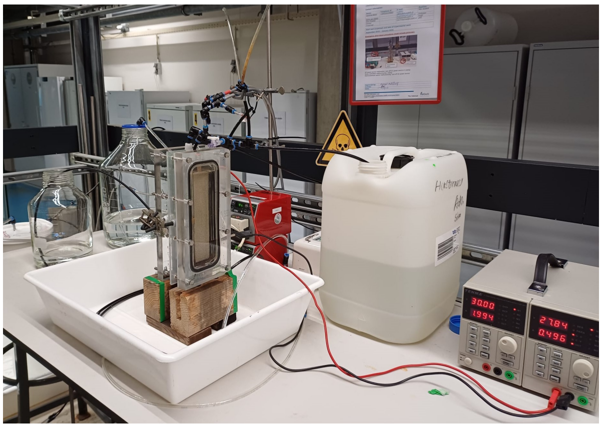

Figure A9.1: TU Delft Laboratory Set-up (RuO_2/IrO_2 depicted in picture)

Figure A9.2: Field setting at Kpeshie Lagoon in Accra, Ghana

Figure A9.3: RuO_2/IrO_2 Reactor

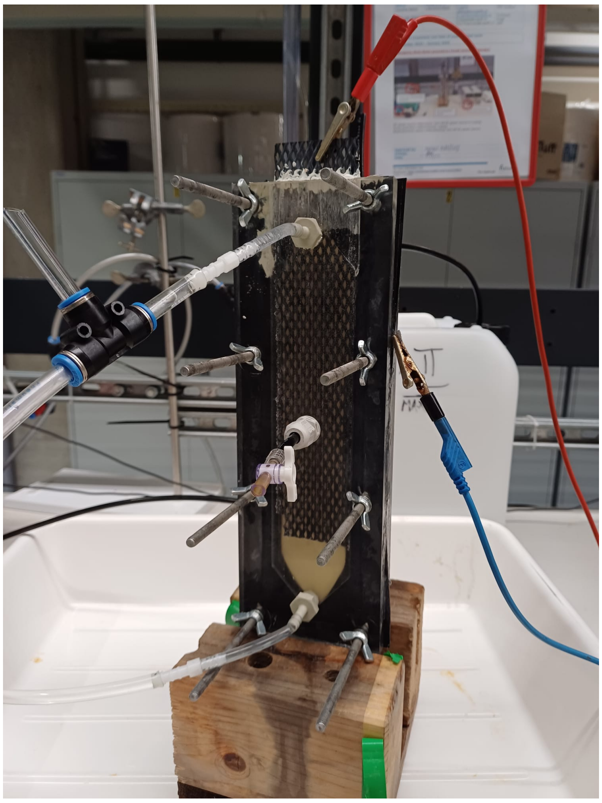

Figure A9.4: Magneli reactor

Bibliography

[1] Chlorine residual. URL `https://dec.vermont.gov/sites/dec/files/wsm/wastewater/docs/Section%209_Total%20Residual%20Chlorine.pdf`. In VT WSMD Wastewater Program Lab Manual Section #9 (pp. 1–12).

[2] Redox chemistry of chlorine & chloramine disinfectants. URL `https://www.sedimentaryores.net/Pipe%20Scales/Chlorine-chloramine.html`.

[3] A. Ahmadi and T. Wu. Inactivation of e. coli using a novel tio2 nanotube electrode. *Environmental Science. Water Research & Technology, 3(3), 534–545.*, 2017. URL `https://doi.org/10.1039/c6ew00319b`.

[4] S. Ahn, T. D. Peterson, J. Righter, D. M. Miles, and P. G. Tratnyek. Disinfection of ballast water with iron activated persulfate. *Environmental Science & Technology, 47(20), 11717–11725.*, 2013. URL `https://doi.org/10.1021/es402508k`.

[5] V. Alfieri. Advanced oxidation processes for water disinfection. *Politecnico di Torino*, 2021. URL `https://webthesis.biblio.polito.it/18761/1/tesi.pdf`.

[6] W. E. I. Andah, N. Van De Giesen, C. A. Biney, and ADAPT. Water, climate, food, and environment in the volta basin. *In Contribution to the Project ADAPT Adaptation Strategies to Changing Environments.* URL `https://weap21.org/downloads/AdaptVolta.pdf`.

[7] Anonymous. Standard electrode potentials. *HyperPhysics.* URL `http://hyperphysics.phy-astr.gsu.edu/hbase/Chemical/electrode.html#c1`.

[8] AQUATABS 167mg tablets. Test All Water: AQUATABS 167mg tablets. URL `https://testallwater.co.uk/products/aquatabs-167mg-tablets?pr_prod_strat=e5_desc&pr_rec_id=aca2239c3&pr_rec_pid=7543674700034&pr_ref_pid=7543856627970&pr_seq=uniform`.

[9] A. Bard and L. Faulkner. *Electrochemical Methods: Fundamentals and Applications.* Wiley Textbooks, 2nd edn, 2000.

[10] H. Bergmann. Electrochemical disinfection – state of the art and tendencies. *Current Opinion in Electrochemistry, 28, 100694.*, 2021. URL `https://doi.org/10.1016/j.coelec.2021.100694`.

[11] B. Bicudo, B. Van Der Werff, G. Medema, and D. Van Halem. Disinfection during iron electrocoagulation: Differentiating between inactivation and floc entrapment for escherichia coli and somatic coliphage Øx174. *ACS ES & T Water, 2(10), 1707–1714.*, 2022. URL `https://doi.org/10.1021/acsestwater.2c00230`.

[12] G. Bitton. *Wastewater microbiology.* New York: Wiley-Liss, 1994. p. 87–92., 1994.

[13] W. Cao, Z. W. Zhu, Z. X. Shi, C. Y. Wang, and B. M. Li. Efficiency of slightly acidic electrolyzed water for inactivation of salmonella enteritidis and its contaminated shell eggs. *International Journal of Food Microbiology, 130(2)*, 2009.

[14] N. Chaukura, S. S. Marais, W. Moyo, N. Mbali, L. C. Thakalekoala, T. Ingwani, B. B. Mamba, P. Jarvis, and T. T. Nkambule. Contemporary issues on the occurrence and removal of disinfection byproducts in drinking water-a review. *Journal of Environmental Chemical Engineering, 8(2), 103659.*, 2020. URL `https://doi.org/10.1016/j.jece.2020.103659`.

[15] C. Comninellis. Electrocatalysis in the electrochemical conversion/combustion of organic pollutants for waste water treatment. *Electrochimica Acta, 39(11–12), 1857–1862.*, 1994. URL `https://doi.org/10.1016/0013-4686(94)85175-1`.

[16] C. Comninellis, A. Kapałka, S. Malato, S. A. Parsons, I. Poulios, and D. Mantzavinos. Advanced oxidation processes for water treatment: advances and trends for r&d. *Journal of Chemical Technology and Biotechnology/Journal of Chemical Technology & Biotechnology, 83(6), 769–776.*, 2008. URL `https://doi.org/10.1002/jctb.1873`.

[17] A Copeland and D. A. Lytle. Measuring the oxidation–reduction potential of important oxidants in drinking water. *Journal of the American Water Works Association/Journal - American Water Works Association, 106(1)*, 2014. URL `https://doi.org/10.5942/jawwa.2014.106.0002`.

[18] Y. Crider, M. Tsuchiya, M Mukundwa, I. Ray, and A. J. Pickering. Adoption of point-of-use chlorination for household drinking water treatment: A systematic review. *Environmental Health Perspectives, 131(1).*, 2023. URL `https://doi.org/10.1289/ehp10839`.

[19] World Bank Open Data. Access to basic drinking water services. Technical report. URL `https://data.worldbank.org/indicator/SH.H2O.BASW.ZS`.

[20] C. P. Davis, M. E. Shirtliff, N. M. Trieff, S. L. Hoskins, and M. M. Warren. Quantification, qualification, and microbial killing efficiencies of antimicrobial chlorine-based substances produced by iontophoresis. *Antimicrobial Agents and Chemotherapy, 38(12), 2768–2774.*, 1994. URL `https://doi.org/10.1128/aac.38.12.2768`.

[21] J. R. Davis, J. C. Baygents, and J. Farrell. Understanding persulfate production at boron doped diamond film anodes. *Electrochimica Acta, 150, 68–74.*, 2014. URL `https://doi.org/10.1016/j.electacta.2014.10.104`.

[22] K. P. Drees, M. Abbaszadegan, and R. M. Maier. Comparative electrochemical inactivation of bacteria and bacteriophage. *Water Research, 37(10), 2291–2300.*, 2003. URL `https://doi.org/10.1016/s0043-1354(03)00009-5`.

[23] L. Dössegger, A. Tournefier, L. Germann, N. Gärtner, T. Huonder, C. Etenu, K. Wanyama, H. Ouma, and R. Meierhofer. Assessment of low-cost, non-electrically powered chlorination devices for gravity-driven membrane water kiosks in eastern uganda. *Waterlines, 40(2), 92–106.*, 2021. URL `https://doi.org/10.3362/1756-3488.20-00014`.

[24] K. Dąbrowska. Phage therapy: What factors shape phage pharmacokinetics and bioavailability? systematic and critical review. *Medicinal Research Reviews, 39(5), 2000–2025.*, 2019. URL `https://doi.org/10.1002/med.21572`.

[25] S. Esposto. On-site electro-chlorination application for water treatment in north iraq. *Water Supply, 9(4), 387–393.*, 2009. URL `https://doi.org/10.2166/ws.2009.392`.

[26] S. O. Ganiyu, C. A. Martínez-Huitle, and M. A. Rodrigo. Renewable energies driven electrochemical wastewater/soil decontamination technologies: A critical review of fundamental concepts and applications. *Applied Catalysis. B, Environmental, 270, 118857.*, 2020. URL `https://doi.org/10.1016/j.apcatb.2020.118857`.

[27] P. Gayen, C. Chen, J. T. Abiade, and B. P. Chaplin. Electrochemical oxidation of atrazine and clothianidin on bi-doped sno2–tino2n–1 electrocatalytic reactive electrochemical membranes. *Environmental Science & Technology, 52(21), 12675–12684.*, 2018. URL `https://doi.org/10.1021/acs.est.8b04103`.

[28] S. Ghasemian, B. Asadishad, S. Omanovic, and N. Tufenkji. Electrochemical disinfection of bacteria-laden water using antimony-doped tin-tungsten-oxide electrodes. *Water Research, 126, 299–307.*, 2017. URL `https://doi.org/10.1016/j.watres.2017.09.029`.

[29] D. Ghernaout. Advanced oxidation phenomena in electrocoagulation process: a myth or a reality? *Desalination and Water Treatment, 51(40–42), 7536–7554.*, 2013. URL `https://doi.org/10.1080/19443994.2013.792520`.

[30] K. E. Gibson. Viral pathogens in water: occurrence, public health impact, and available control strategies. *Current Opinion in Virology, 4, 50–57.*, 2014.

[31] M. Grzegorzek, K. Wartalska, and B. Kaźmierczak. Review of water treatment methods with a focus on energy consumption. *International Communications in Heat and Mass Transfer, 143, 106674.*, 2023. URL `https://doi.org/10.1016/j.icheatmasstransfer.2023.106674`.

[32] Charles N. Haas, Joan B. Rose, Charles Gerba, and Stig Regli. Risk assessment of virus in drinking water. *Risk Analysis, 13(5), 545–552.*, 1993.

[33] S. Hand and R. D. Cusick. Electrochemical disinfection in water and wastewater treatment: Identifying impacts of water quality and operating conditions on performance. *Environmental Science & Technology, 55(6), 3470–3482.*, 2021.

[34] J. G. Jacangelo, V. P. Olivieri, and K. Kawata. Thiosulfate-dechlorination interference with the folin-ciocalteu reagent method for protein determination. *Water Research, 21(9), 1143–1144*, 1987.

[35] J. Jeong, J. Y. Kim, and J. Yoon. The role of reactive oxygen species in the electrochemical inactivation of microorganisms. *Environmental Science & Technology, 40(19), 6117–6122.*, 2006. URL `https://doi.org/10.1021/es0604313`.

[36] J. Jeong, C. Kim, and J. Yoon. The effect of electrode material on the generation of oxidants and microbial inactivation in the electrochemical disinfection processes. *Water Research, 43(4), 895–901.*, 2009. URL `https://doi.org/10.1016/j.watres.2008.11.033`.

[37] E. Jończyk, M. Kłak, R. Międzybrodzki, and A. Górski. The influence of external factors on bacteriophages—review. *Folia Microbiologica, 56(3), 191–200.*, 2011. URL `https://doi.org/10.1007/s12223-011-0039-8`.

[38] Y. J. Jung, K. W. Baek, B. S. Oh, and J. Kang. An investigation of the formation of chlorate and perchlorate during electrolysis using pt/ti electrodes: The effects of ph and reactive oxygen species and the results of kinetic studies. *Water Research, 44(18), 5345–5355.*, 2010. URL `https://doi.org/10.1016/j.watres.2010.06.029`.

[39] H. Kashiwase and T. Fujs. World water day: Two billion people still lack access to safely managed water. *World Bank Blogs*, 2023. URL `https://blogs.worldbank.org/opendata/world-water-day-two-billion-people-still-lack-access-safely-managed-water`.

[40] P. A. Kempler and A. C. Nielander. Reliable reporting of faradaic efficiencies for electrocatalysis research. *Nature Communications, 14(1)*, 2023.

[41] J. Kim, C. W. Lee, and J. Yoon. Electrochemical peroxodisulfate (pds) generation on a self-doped tio2 nanotube array electrode. *Industrial & Engineering Chemistry Research, 57(33), 11465–11471.*, 2018. URL `https://doi.org/10.1021/acs.iecr.8b01208`.

[42] Y. Kott, E. Nupen, and W. R. Ross. The effect of ph on the efficiency of chlorine disinfection and virus enumeration. *Water Research, 9(10), 869–872.*, 1975. URL `https://doi.org/10.1016/0043-1354(75)90034-2`.

[43] E. Kraaijeveld, S. Rijsdijk, S. van der Poel, J.P. van der Hoek, K. Rabaey, and D. van Halem. Electrochemical arsenite oxidation for drinking water treatment: Mechanisms, by-product formation and energy consumption. *Water Research, 253, 121227*, 2024. URL `https://doi.org/10.1016/j.watres.2024.121227`.

[44] A Kraft. Electrochemical water disinfection: A short review. *Platinum Metals Review, 52(3), 177–185.*, 2008.

[45] A. V. Kulinkina, K. C. Kosinski, A. Liss, M. N. Adjei, G. A. Ayamgah, P. Webb, D. M. Gute, J. D. Plummer, and E. N. Naumova. Piped water consumption in ghana: A case study of temporal and spatial patterns of clean water demand relative to alternative water sources in rural small towns. *Science of the Total Environment, 559, 291–301.*, 2016. URL `https://doi.org/10.1016/j.scitotenv.2016.03.148`.

[46] P. Kumar, R. P. Bharti, V. Kumar, and P. P. Kundu. Polymer electrolyte membranes for microbial fuel cells: Part a. nafion-based membranes. *In Elsevier eBooks (pp. 47–72).*, 2018. URL `https://doi.org/10.1016/b978-0-444-64017-8.00004-x`.

[47] W. Li, J. Lin, and C. Huang. The electrochemical kinetics of chloride oxidation over multi-metallic pt-ni-co electrodes affected by metal deposition method and electrode support. *Electrochimica Acta, 469, 143294.*, 2023. URL `https://doi.org/10.1016/j.electacta.2023.143294`.

[48] Z. Li, D. Yang, S. Li, Y. Liu, W. Yan, and H. Xu. Advances on electrochemical disinfection research: Mechanisms, influencing factors and applications. *Science of the Total Environment, 912, 169043.*, 2024. URL `https://doi.org/10.1016/j.scitotenv.2023.169043`.

[49] S. Liang, H. Lin, M. Y. Habteselassie, and Q. Huang. Electrochemical inactivation of bacteria with a titanium sub-oxide reactive membrane. *Water Research, 145, 172–180.*, 2018. URL `https://doi.org/10.1016/j.watres.2018.08.010`.

[50] C. Lin, R. Zhang, S. A. Waisner, T. Nawaz, L. Center, D. B. Gent, J. W. Johnson, and S. Holland. Effects of process factors on the performance of electrochemical disinfection for wastewater in a continuous-flow cell reactor. *Environmental Science and Pollution Research*, 28(27):36573–36584, 2021.

[51] M. Lin, D. M. Bulman, C. K. Remucal, and B. P. Chaplin. Chlorinated byproduct formation during the electrochemical advanced oxidation process at magnéli phase ti4o7 electrodes. *Environmental Science & Technology, 54(19), 12673–12683.*, 2020. URL `https://doi.org/10.1021/acs.est.0c03916`.

[52] M. Lindmark, K. Cherukumilli, Y. Crider, P. Marcenac, M. Lozier, L. E. Voth-Gaeddert, D. Lantagne, J. R. Mihelcic, Q. M. Zhang, C. L. Just, and A. J. Pickering. Passive in-line chlorination for drinking water disinfection: A critical review. *Environmental Science & Technology, 56(13), 9164–9181.*, 2022. URL `https://doi.org/10.1021/acs.est.1c08580`.

[53] W. Brown Liu, M. R. W., and T. Elliott. Mechanisms of the bactericidal activity of low amperage electric current (dc). *the Journal of Antimicrobial Chemotherapy/Journal of Antimicrobial Chemotherapy, 39(6), 687–695.*, 1997. URL `https://doi.org/10.1093/jac/39.6.687`.

[54] X. Liu, C.N. Song, Y. Zhang, L. Sha, Y. Li, and S. Zhang. Electrochemical pretreatment of coking wastewater by ti/btn/ruo2-iro2-tio2: selectivity of chloridion oxidation and multi-response optimization. *Separation and Purification Technology, 276, 119229.*, 2021. URL `https://doi.org/10.1016/j.seppur.2021.119229`.

[55] M. Luna-Trujillo, R. E. Palma-Goyes, J. Vázquez-Arenas, and A. Manzo-Robledo. Formation of active chlorine species involving the higher oxide mox+1 on active ti/ruo2-iro2 anodes: A dems analysis. *Journal of Electroanalytical Chemistry, 878, 114661.*, 2020.

[56] T. Léziart, P. D. De La Rochere, R. Cheswick, P. Jarvis, and A. Nocker. Effect of turbidity on water disinfection by chlorination with the emphasis on humic acids and chalk. *Environmental Technology, 40(13), 1734–1743*, 2019. URL `https://doi.org/10.1080/09593330.2019.1585480`.

[57] G. R. P. Malpass and A. J. Motheo. Recent advances on the use of active anodes in environmental electrochemistry. *Current Opinion in Electrochemistry, 27, 100689.*, 2021. URL `https://doi.org/10.1016/j.coelec.2021.100689`.

[58] B. Marselli, J. Garcıá-Gómez, P. Michaud, M. A. Rodrigo, and C. Comninellis. Electrogeneration of hydroxyl radicals on boron-doped diamond electrodes. *Journal of the Electrochemical Society*, 150(3):D79, 2003. URL `https://doi.org/10.1149/1.1553790`.

[59] C. A. Martínez-Huitle, M. A. Rodrigo, I. Sirés, and O. Scialdone. Single and coupled electrochemical processes and reactors for the abatement of organic water pollutants: A critical review. *Chemical Reviews, 115(24), 13362–13407.*, 2015. URL `https://doi.org/10.1021/acs.chemrev.5b00361`.

[60] C. A. Martínez-Huitle and L. S. Andrade. Electrocatalysis in wastewater treatment: recent mechanism advances. *Química Nova, 34(5), 850–858.*, 2011. URL `https://doi.org/10.1590/s0100-40422011000500021`.

[61] C. A. Martínez-Huitle and E. Brillas. Electrochemical alternatives for drinking water disinfection. *Angewandte Chemie, 47(11), 1998–2005.*, 2008. URL `https://doi.org/10.1002/anie.200703621`.

[62] C. A. Martínez-Huitle and S. Ferro. Electrochemical oxidation of organic pollutants for the wastewater treatment: direct and indirect processes. *Chem Inform, 38(14).*, 2007. URL `https://doi.org/10.1002/chin.200714276`.

[63] T. Matsunaga, S. Nakasono, Y. Kitajima, and K. Horiguchi. Electrochemical disinfection of bacteria in drinking water using activated carbon fibers. *Biotechnology and Bioengineering, 43(5), 429–433.*, 1994. URL `https://doi.org/10.1002/bit.260430511`.

[64] F. V. Mehendale, G. Clayton, K. M. Homyer, and D. M. Reynolds. Hocl vs ocl-: clarification on chlorine-based disinfectants used within clinical settings. *Journal of Global Health Reports, 7*, 2023. URL `https://doi.org/10.29392/001c.84488`.

[65] A. Michel, O. Clermont, E. Denamur, and O. Tenaillon. Bacteriophage phix174's ecological niche and the flexibility of its escherichia coli lipopolysaccharide receptor. *Applied and Environmental Microbiology, 76(21), 7310–7313.*, 2010.

[66] A. Miller, L. Singh, L. Wang, and H. Liu. Linking internal resistance with design and operation decisions in microbial electrolysis cells. *Environment International, 126, 611–618.*, 2019. URL `https://doi.org/10.1016/j.envint.2019.02.056`.

[67] Moreno-Andrés, Farinango J., L. G., Romero-Martínez, A. Acevedo-Merino, and E. Nebot. Application of persulfate salts for enhancing uv disinfection in marine waters. *Water Research, 163, 114866.*, 2019. URL `https://doi.org/10.1016/j.watres.2019.114866`.

[68] J. K. Fawell Mr., J. Cotruvo, M. Giddings, P. Jackson, Y. Magara, E. Ohanian, and World Health Organization. ph in drinking-water. *Revised Background Document for Development of WHO Guidelines for Drinking-water Quality.*, 2007. URL `https://cdn.who.int/media/docs/default-source/wash-documents/wash-chemicals/ph.pdf?sfvrsn=16b10656_4`.

[69] A. Muthurasu and V. Ganesh. Electrochemical characterization of self-assembled monolayers (sams) of silanes on indium tin oxide (ito) electrodes – tuning electron transfer behaviour across electrode–electrolyte interface. *Journal of Colloid and Interface Science, 374(1), 241–249.*, 2012. URL `https://doi.org/10.1016/j.jcis.2012.02.007`.

[70] S. Nappier, Inc. ICF International, Versar, V. J. Harwood, S. Jiang, M. D. Sobsey, S. Nappier, A. Ichida, K. Jaglo, J. Soller, A. Varghese, A. Boehm, K. Nelson, M. Nellor, and K. Jones. Review of coliphages as possible indicators of fecal contamination for ambient water quality. *In J. Strong & E. Doyle (Eds.), EPA Office of Water (No. 820-R-15–098).*, 2015.

[71] G. Norra, L. Baptista-Pires, E. C. Lumbaque, C. M. Borrego, and J. Radjenovic. Chlorine-free electrochemical disinfection using graphene sponge electrodes. *Chemical Engineering Journal, 430, 132772.*, 2022. URL `https://doi.org/10.1016/j.cej.2021.132772`.

[72] E. Nurhayati. A brief review on electro-generated hydroxyl radical for organic wastewater mineralization. *Jurnal Sains Dan Teknologi Lingkungan/Jurnal Sains & Teknologi Lingkungan, 4(1), 24–31.*, 2012. URL `https://doi.org/10.20885/jstl.vol4.iss1.art3`.

[73] UNICEF Division of Global Communication and Advocacy. Triple threat: How disease, climate risks, and unsafe water, sanitation and hygiene create a deadly combination for children. *UNICEF. https://www.unicef.org/media/137206/file/triple-threat-wash-EN.pdf*, 2023.

[74] World Health Organization. *Guidelines for drinking-water quality [Book]. In WHO Library Cataloguing-in-Publication Data (FOURTH EDITION).* 2011.

[75] World Health Organization. Principles and practices of drinking-water chlorination: A guide to strengthening chlorination practices in small- to medium-sized water supplies. 2017.

[76] R. E. Palma-Goyes, F. L. Guzmán-Duque, G. A. Peñuela, I. González, J. L. Nava, and R. A. Torres-Palma. Electrochemical degradation of crystal violet with bdd electrodes: Effect of electrochemical parameters and identification of organic by-products. *Chemosphere, 81(1), 26–32.*, 2010. URL `https://doi.org/10.1016/j.chemosphere.2010.07.020`.

[77] J. M. Peralta-Hernández, M. Méndez-Tovar, R. J. Guerra-Sánchez, C. A. Martínez-Huitle, and J. L. Nava. A brief review on environmental application of boron doped diamond electrodes as a new way for electrochemical incineration of synthetic dyes. *International Journal of Electrochemistry, 2012, 1–18.*, 2012. URL `https://doi.org/10.1155/2012/154316`.

[78] A. Polcaro, A. Vacca, M. Mascia, S. Palmas, and J. R. Ruiz. Electrochemical treatment of waters with bdd anodes: kinetics of the reactions involving chlorides. *ournal of Applied Electrochemistry, 39(11), 2083–2092.*, 2009. URL `https://doi.org/10.1007/s10800-009-9870-x`.

[79] G. Pérez, P. C. Gómez, R. Ibáñez, I. Ortiz, and A. Urtiaga. Electrochemical disinfection of secondary wastewater treatment plant (wwtp) effluent. *Water Science & Technology, 62(4), 892–897.*, 2010. URL `https://doi.org/10.2166/wst.2010.328`.

[80] A. R. Rahmani, M. R. Samarghandi, D. Nematollahi, and F. Zamani. A comprehensive study of electrochemical disinfection of water using direct and indirect oxidation processes. *ournal of Environmental Chemical Engineering, 7(1), 102785.*, 2019. URL `https://doi.org/10.1016/j.jece.2018.11.030`.

[81] M. Rajab, C. Heim, T. Letzel, J. E. Drewes, and B. Helmreich. Electrochemical disinfection using boron-doped diamond electrode – the synergetic effects of in situ ozone and free chlorine generation. *Chemosphere, 121, 47–53.*, 2015. URL `https://doi.org/10.1016/j.chemosphere.2014.10.075`.

[82] B. Reed. Technical notes on drinking-water, sanitation and hygiene in emergencies: Measuring chlorine levels in water supplies. *WHO*, 2013.

[83] S. Rijsdijk. Exploring electrochemical advanced oxidation processes as novel method for arsenic removal from dune water. 2022.

[84] H. Rossiter, P. A. Owusu, E. Awuah, A. MacDonald, and A. Schäfer. Chemical drinking water quality in ghana: Water costs and scope for advanced treatment. *Science of the Total Environment, 408(11), 2378–2386.*, 2010. URL `https://doi.org/10.1016/j.scitotenv.2010.01.053`.

[85] J. P. Saha and S. K. Gupta. A novel electro-chlorinator using low cost graphite electrode for drinking water disinfection. *Ionics, 23(7), 1903–1913.*, 2017. URL `https://doi.org/10.1007/s11581-017-2022-0`.

[86] M. A. Sandoval, W. Calzadilla, and R. Salazar. Influence of reactor design on the electrochemical oxidation and disinfection of wastewaters using boron-doped diamond electrodes. *Current Opinion in Electrochemistry, 33, 100939.*, 2022.

[87] C. Schillings, R. Meyer, F. Trieb, and Deutsches Zentrum für Luft-und Raumfahrt. High resolution solar radiation assessment for ghana. *In SWERA.*, 2004. URL `https://openei.org/datasets/files/710/pub/ghana_10km_solar_country_report.pdf`.

[88] R. Sharifian, R. M. Wagterveld, I. A. Digdaya, C. Xiang, and D. A. Vermaas. Electrochemical carbon dioxide capture to close the carbon cycle. *Energy & Environmental Science, 14(2), 781–814.*, 2021. URL `https://doi.org/10.1039/d0ee03382k`.

[89] Y Shevah. Adaptation to water scarcity and regional cooperation in the middle east. *Elsevier eBooks (pp. 40–70). https://doi.org/10.1016/b978-0-12-382182-9.00004-9*, 2014.

[90] Y.J. Shih, C.C. Su, M.C. Lu, and C.P. Huang. The electrodeless preparation of m (m = pt, pd, ru, cu) ni-co oxide/graphite electrodes for the electrochemical inactivation of escherichia coli. *Sustainable Environment Research, 26(1), 1–13.*, 2016. URL `https://doi.org/10.1016/j.serj.2016.01.001`.

[91] S. K. Singh, P. Robert, and F. Hassard. Coliphages as viral indicators of sanitary significance for drinking water. *Frontiers in Microbiology, 13.*, 2022.

[92] I. Sirés, E. Brillas, M. A. Oturan, M. A. Rodrigo, and M. Panizza. Electrochemical advanced oxidation processes: today and tomorrow. a review. *Environmental Science and Pollution Research International, 21(14), 8336–8367.*, 2014. URL `https://doi.org/10.1007/s11356-014-2783-1`.

[93] M. Sobsey, J. Brown, and World Health Organization. *Evaluating household water treatment options: health-based targets and microbiological performance specifications.* World Health Organization, 2011.

[94] A. Soodan. Electrochemical reduction for metal recovery in water treatment: A novel approach. 2023. URL `http://resolver.tudelft.nl/uuid:2146c9bf-c5ad-4c79-9790-8a5b3c150ec9`.

[95] Statista. Prices of electricity in ghana 2023, by user. *Statista*, 2024.

[96] R. Stirling, W. S. Walker, P. Westerhoff, and S. Garcia-Segura. Techno-economic analysis to identify key innovations required for electrochemical oxidation as point-of-use treatment systems. *Electrochimica Acta*, 338:135874, 2020. URL `https://doi.org/10.1016/j.electacta.2020.135874`.

[97] C. Trellu, B. P. Chaplin, C. Coetsier, R. Esmilaire, S. Cerneaux, C. Causserand, and M. Cretin. Electro-oxidation of organic pollutants by reactive electrochemical membranes. *Chemosphere, 208, 159–175.*, 2018. URL `https://doi.org/10.1016/j.chemosphere.2018.05.026`.

[98] S. A. Trikannad, D. Van Halem, J. W. Foppen, and J. P. Van Der Hoek. The contribution of deeper layers in slow sand filters to pathogens removal. *Water Research, 237, 119994.*, 2023.

[99] D. Trogolo and J. S.) Arey. Equilibria and speciation of chloramines, bromamines, and bromochloramines in water. *Environmental Science & Technology, 51(1), 128–140.*, 2016. URL `https://doi.org/10.1021/acs.est.6b03219`.

[100] L. Venczel, M. J. Arrowood, M. R. Hurd, and M. D. Sobsey. Inactivation of cryptosporidium parvum oocysts and clostridium perfringens spores by a mixed-oxidant disinfectant and by free chlorine. *Applied and Environmental Microbiology, 63(4), 1598–1601.*, 1997. URL `https://doi.org/10.1128/aem.63.4.1598-1601.1997`.

[101] C.M. Villanueva, S. Cordier, L. Font-Ribera, L.A. Salas, and P. Levallois. Overview of disinfection by-products and associated health effects. *Current Environmental Health Reports, 2(1), 107–115.*, 2015. URL `https://doi.org/10.1007/s40572-014-0032-x`.

[102] M. Von Sperling, M. E. von, Verbyla, S. M. a. C. Oliveira, and The Authors. *Chapter 7: Removal efficiencies. In Assessment of Treatment Plant Performance and Water Quality Data: A Guide for Students, Researchers and Practitioners.* 2020.

[103] L. Wang, Y. Chen, F. Long, L. Singh, S. Trujillo, X. Xiao, and H. Liu. Breaking the loop: Tackling homoacetogenesis by chloroform to halt hydrogen production-consumption loop in single chamber microbial electrolysis cells. *Chemical Engineering Journal, 389, 124436.*, 2020. URL `https://doi.org/10.1016/j.cej.2020.124436`.

[104] L. Wang, Y. Wang, Y. Sui, J. Lu, B. Hu, and Q. Huang. Formation of chlorate and perchlorate during electrochemical oxidation by magnéli phase ti4o7 anode: inhibitory effects of coexisting constituents. *Scientific Reports, 12(1).*, 2022. URL `https://doi.org/10.1038/s41598-022-19310-5`.

[105] D. N. Wordofa, S. L. Walker, and H. Liu. Sulfate radical-induced disinfection of pathogenic escherichia coli o157:h7 via iron-activated persulfate. *Environmental Science & Technology Letters, 4(4), 154–160.*, 2017. URL `https://doi.org/10.1021/acs.estlett.7b00035`.

[106] K. Xiang, Z. Song, D. Wu, X. Deng, X. Wang, W. Yan, Z. Peng, L. Wang, J. Luo, and X. Fu. Bifunctional pt–co3o4 electrocatalysts for simultaneous generation of hydrogen and formate via energy-saving alkaline seawater/methanol co-electrolysis. *Journal of Materials Chemistry. A, 9(10), 6316–6324.*, 2021. URL `https://doi.org/10.1039/d0ta10501e`.

[107] J. Xie, J. Ma, S. Zhao, and T. D. Waite. Flow anodic oxidation: Towards high-efficiency removal of aqueous contaminants by adsorbed hydroxyl radicals at 1.5 v vs she. *Water Research, 200, 117259.*, 2021. URL `https://doi.org/10.1016/j.watres.2021.117259`.

[108] J. Xie, C. Zhang, and T. D. Waite. Hydroxyl radicals in anodic oxidation systems: generation, identification and quantification. *Water Research, 217, 118425.*, 2022. URL `https://doi.org/10.1016/j.watres.2022.118425`.

[109] Haoran Xu and Meng Ni. *Hybrid Energy System models.* ScienceDirect, 2020. URL `https://www.sciencedirect.com/book/9780128214039/hybrid-energy-system-models`.

[110] E. Yeleliere, S. J. Cobbina, and A. B. Duwiejuah. Review of ghana's water resources: the quality and management with particular focus on freshwater resources. *Applied Water Science, 8(3).*, 2018. URL `https://doi.org/10.1007/s13201-018-0736-4`.

[111] J. Yin, S. Almassi, S. Mehraeen, R. J. LeSuer, and B. P. Chaplin. The roles of oxygen vacancies, electrolyte composition, lattice structure, and doping density on the electrochemical reactivity of magnéli phase tio2anodes. *Journal of Materials Chemistry. A, 6(46), 23828–23839.*, 2018. URL `https://doi.org/10.1039/c8ta03719a`.

[112] M. Gao Yu, X. R. Lv, M. Sui, and L. Tian. Inactivation of phage phix174 by uv254 and free chlorine: Structure impairment and function loss. *Journal of Environmental Management, 340, 117962.*, 2023.

[113] X. Zeng, M. Zhang, X. Wang, X. Chen, X. Su, and W. Tang. Effects of sn content on ti/ruo2-sno2-tio2 anodes used in the generation of electrolyzed oxidizing water. *Journal of Electroanalytical Chemistry, 677–680, 133–138.*, 2012. URL `https://doi.org/10.1016/j.jelechem.2012.05.008`.

[114] J. Zhang, P. Su, T. Xu, L. Yuan, M. Qiao, B. Yang, and Y. Wang. Comprehensive study on the role of reactive oxygen species and active chlorine species on the inactivation and subcellular damage of e.coli in electrochemical disinfection. *Separation and Purification Technology, 304, 122408.*, 2023. URL `https://doi.org/10.1016/j.seppur.2022.122408`.

[115] A. R. Žeradjanin, N. Menzel, W. Schuhmann, and P. Strasser. On the faradaic selectivity and the role of surface inhomogeneity during the chlorine evolution reaction on ternary ti–ru–ir mixed metal oxide electrocatalysts. *Physical Chemistry Chemical Physics/PCCP. Physical Chemistry Chemical Physics, 16(27), 13741–13747.*, 2014. URL `https://doi.org/10.1039/c4cp00896k`.